Organic geochemistry and petrology of sedimentary exhalative Pb-Zn and polymetallic hyper-enriched black shale deposits in the Selwyn Basin, Yukon

J.M. Peter[1]*, M.G. Gadd[1], C. Jiang[2], and J. Reyes[2]

Peter, J.M., Gadd, M.G., Jiang, C., and Reyes, J., 2022. Organic geochemistry and petrology of sedimentary exhalative Pb-Zn and polymetallic hyper-enriched black shale deposits in the Selwyn Basin, Yukon; in *Targeted Geoscience Initiative 5: volcanic- and sediment-hosted massive-sulfide deposit genesis and exploration methods, (ed.) J.M. Peter and M.G. Gadd; Geological Survey of Canada, Bulletin 617, p. 89–112. https://doi.org/10.4095/328017*

Abstract: Paleozoic strata of the Selwyn Basin host sedimentary exhalative (SEDEX) Pb-Zn deposits, and age-correlative strata of the Richardson trough host polymetallic hyper-enriched black shale (HEBS) deposits. In both deposit types, organic matter is spatially and temporally associated with mineralization. We investigated the characteristics of organic matter in mineralization and unmineralized host rocks in the XY Central SEDEX deposit in the Howard's Pass district, and the Nick and Peel River HEBS deposits in the Richardson trough using Rock-Eval pyrolysis, organic petrography, and solvent extraction and gas chromatography mass spectrometry (GCMS) analysis of the soluble organic matter (SOM). All samples experienced extremely high thermal maturity (T_{max} up to 599°C), indicating they contain low SOM. Rock-Eval parameters S1, S2, HI, and OI values are low. Total organic carbon (TOC) values are low for Nick and Peel River and are generally higher for XY Central. Residual carbon values are universally high. Mineral carbon values are low for deposits studied (one outlier). Pyrobitumen reflectance is mostly below 5.80%. Full-scan GCMS analyses of SOM reveal that most, if not all, high molecular weight hydrocarbons, including biomarkers, have been lost due to thermal cracking and many detected peaks are likely due to contaminants introduced during sampling.

Résumé : Les strates paléozoïques du bassin de Selwyn renferment des gîtes exhalatifs de Pb-Zn dans des roches sédimentaires (gîtes SEDEX), tandis que les strates d'âge corrélatif de la cuvette de Richardson renferment des gîtes de shales noirs surenrichis à minéralisation polymétallique. Dans les deux types de gîtes, de la matière organique est associée de façon spatiale et temporelle à la minéralisation. Au moyen de la pyrolyse Rock-Eval, de la pétrographie organique et de l'analyse de la matière organique soluble par extraction à l'aide de solvants et chromatographie en phase gazeuse couplée à la spectrométrie de masse (GC-MS), nous avons étudié les caractéristiques de la matière organique dans la minéralisation et les roches hôtes non minéralisées du gîte SEDEX de XY Central, dans le district de Howard's Pass, et des gîtes de shales noirs surenrichis de Nick et de Peel River, dans la cuvette de Richardson. Tous les échantillons présentent une maturité thermique extrêmement élevée (T_{max} jusqu'à 599 °C), ce qui signifie qu'ils contiennent peu de matière organique soluble. Les valeurs des paramètres S1, S2, IH et IO de la pyrolyse Rock-Eval sont faibles. Les concentrations de carbone organique total (COT) sont faibles pour les gîtes de Nick et de Peel River et généralement plus élevées pour le gîte de XY Central, tandis que les concentrations de carbone résiduel sont élevées partout. Les valeurs de la concentration de carbone minéral sont faibles pour les gîtes étudiés (sauf une valeur aberrante). La réflectance du pyrobitume est essentiellement inférieure à 5,80 %. Les analyses par balayage complet de la matière organique soluble par GC-MS révèlent que la plupart, sinon la totalité, des hydrocarbures à poids moléculaire élevé, y compris les biomarqueurs, ont disparu en raison du craquage thermique et que les nombreux pics détectés sont probablement causés par des contaminants introduits au moment de l'échantillonnage.

[1]Geological Survey of Canada, 601 Booth Street, Ottawa, Ontario K1A 0E8
[2]Geological Survey of Canada, 3303 33rd Street NW, Calgary, Alberta T2L 2A7
*Corresponding author: J.M. Peter (email: jan.peter@nrcan-rncan.gc.ca)

INTRODUCTION

The Selwyn Basin is a large, northwest-trending, Paleozoic deep-water sedimentary basin mainly composed of Ordovician to Devonian black shale and chert, and it extends for thousands of kilometres from Alaska through Yukon and western Northwest Territories, and into northern British Columbia (Fig. 1; Goodfellow, 2007). The Selwyn Basin hosts sedimentary exhalative (SEDEX) Pb-Zn and polymetallic hyper-enriched black shale (HEBS) deposits (Fig. 1). These deposit types show strong spatial and temporal correlation with abundant organic matter (e.g. Coveney, 1997; Pratt and Warner, 1997). This organic matter may play a passive (bystander) or an integral role in the mineralizingprocess (Leventhal and Giordano, 1997). For example, at several SEDEX deposits in the Selwyn Basin, metals are thought to have been fixed by anaerobic oxidation of methane coupled to organic-matter–driven bacterial sulfate reduction (BSR) at the sulfate-methane transition zone (Magnall et al., 2016; Johnson et al., 2018). During BSR, microbes consume labile organic matter through dissolved sulfate respiration (Goldhaber and Kaplan, 1980), and the reduced sulfur fixes available metals. This process has also been proposed to fix metals in HEBS (Gadd, Peter, and Layton-Matthews, this volume).

Whether directly or indirectly involved in the mineralizing processes, the character and origin of organic matter may provide information about the paleoenvironment in which the deposits formed (Peters et al., 2005). The salient goal of our research was to determine the role and significance of micro-organisms in the formation of deposits hosted in carbonaceous sediments. Although negative sulfur isotope compositions in sulfide minerals provide clear evidence of active and intense BSR, the site of this process (confined to sediments below the sediment-water interface or migrated into the water column) is unclear (Gadd et al., 2017; Gadd, Peter, and Layton-Matthews, this volume). Traditional models of both SEDEX and HEBS stipulate euxinic conditions, implying BSR within the ambient water column (e.g. Goodfellow, 2007). Evidence for this is generally equivocal, but organic petrological and geochemical analyses may be revelatory in establishing the role and extent of euxinia (Holman et al., 2014a, b, c).

To investigate the role of organic matter in the mineralizing processes, we studied the characteristics organic matter in the mineralized strata and unmineralized host rocks of one SEDEX deposit (XY Central) in the Howard's Pass district, and two HEBS deposits (Nick and Peel River), all within the Selwyn Basin and correlative strata of the Richardson trough (Fig. 1). We subjected samples of shale, mudstone, and pyrobitumen to Rock-Eval pyrolysis and petrographic examination to evaluate bulk organic properties, then completed solvent extraction and gas chromatography mass spectrometry (GCMS) analyses for molecular fingerprinting of soluble organic matter (SOM).

GEOLOGY

The Selwyn Basin is a large, elongated continental margin sedimentary basin situated at the western margin of ancestral North America. It extends from Alaska through Yukon, Northwest Territories, and British Columbia. The basin is flanked along the east and west margins by the Mackenzie and Macdonald carbonate platforms, respectively (Fig. 1). The basin hosts a complete sedimentary architecture: Late Proterozoic syn-rift clastic rocks of the Windermere Supergroup comprising predominantly oxidized, coarse- and fine-grained clastic rocks of local derivation (Eisbacher, 1981) and a Paleozoic sag or post-rift sedimentary sequence composed mostly of black and carbonaceous pelagic and hemipelagic shale and chert (Goodfellow, 2007; Strauss et al., 2020). These strata are Cambrian to Ordovician carbonate rocks of the Rabbitkettle Formation, overlain by basinal facies chert and shale of the Ordovician to Devonian Road River Group and chert and autochthonous black clastic rocks of the Devonian to Mississippian Earn Group (Gordey et al., 1988). Sedimentation of these rocks ended with the deposition of the Imperial Formation of the Devonian clastic wedge, which prograded in front of the advancing Ellesmerian Orogeny (Pugh, 1983; Lane, 2007). The western margin of the Selwyn Basin has been interpreted as the outer margin of the Proterozoic continental margin (Nelson and Colpron, 2007). The Selwyn Basin's northwest-trending fold and thrust faults were formed by northeast-directed horizontal compression, presumably following a thin-skinned detachment model (Gordey and Anderson, 1993). The metamorphic grade is sub-greenschist, and peak metamorphism and deformation is estimated to have occurred 170 ± 20 Ma (*see* Kawasaki et al., 2012).

Howard's Pass district and XY Central SEDEX deposit

The Howard's Pass district of the Selwyn Basin (Fig. 1) hosts world-class SEDEX Zn-Pb deposits (Goodfellow, 2007). The geology of the Howard's Pass district is detailed in Gadd et al. (2016) and the stratigraphy is summarized in Figure 2. Mineralization in the Howard's Pass district is restricted to the Ordovician to Silurian Duo Lake Formation of the Road River Group, which comprises carbonaceous, siliceous, and calcareous mudstone; cherty mudstone; and minor limestone. The Duo Lake Formation has been informally subdivided into several distinct lithological members at Howard's Pass (Morganti, 1979). These are the Pyritic Siliceous Mudstone member; the Lower Cherty Mudstone member; and the Calcareous Carbonaceous Mudstone member, which together constitute the immediate stratigraphic footwall to the mineralization; the Active member , which hosts the mineralization; and the Upper Siliceous Mudstone member, which forms the immediate stratigraphic hanging wall to the mineralization.

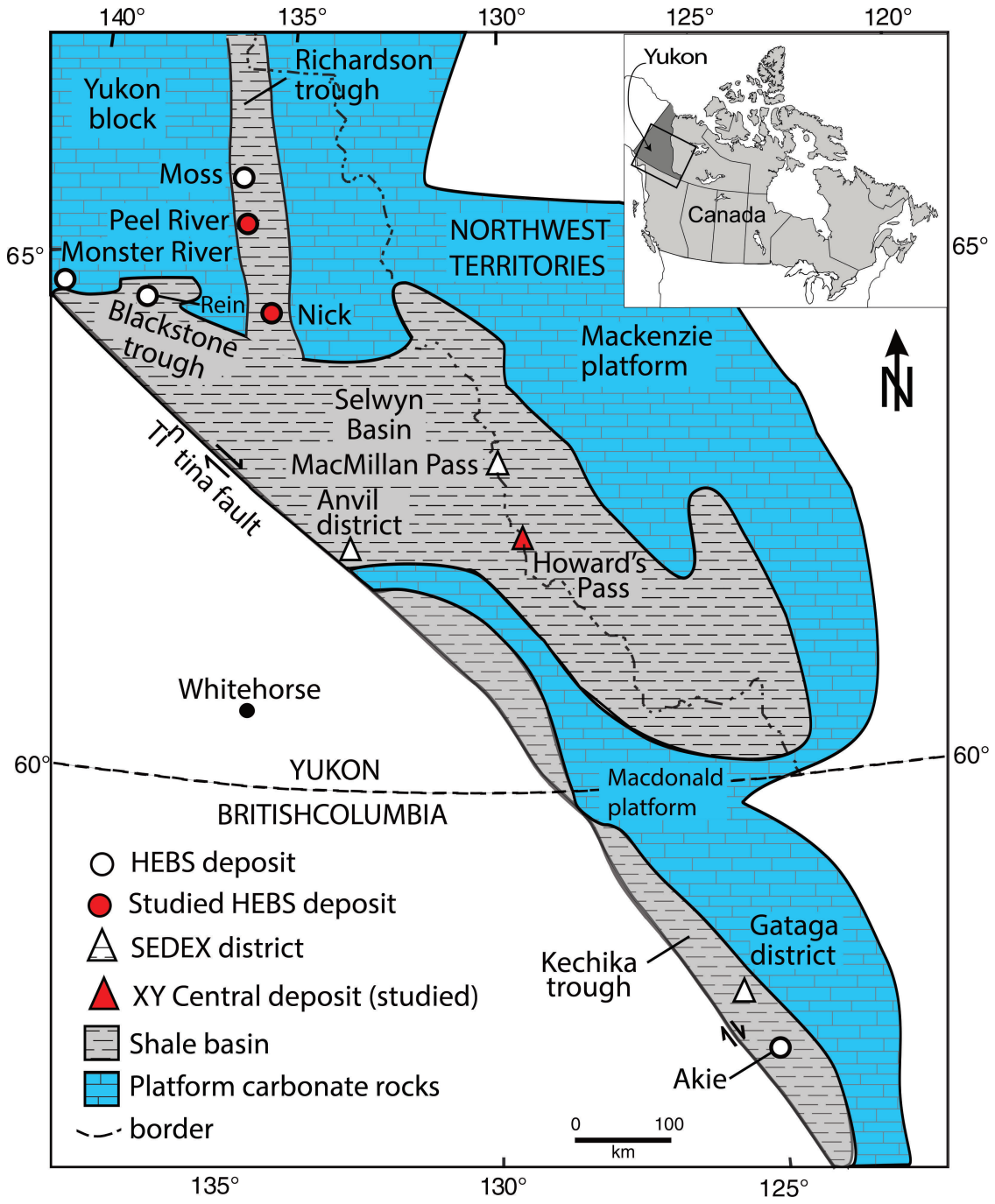

Figure 1. General geological map of the Selwyn Basin and Mackenzie platform, Yukon, showing major sedimentary exhalative (SEDEX) Zn-Pb-(Ag-Ba) districts and hyper-enriched black shale (HEBS) deposits (*modified from* Gadd, Peter, and Layton-Matthews, this volume). Red-filled symbols denote deposit sites sampled (XY Central, the Howard's Pass district; Nick and Peel River, Richardson trough).

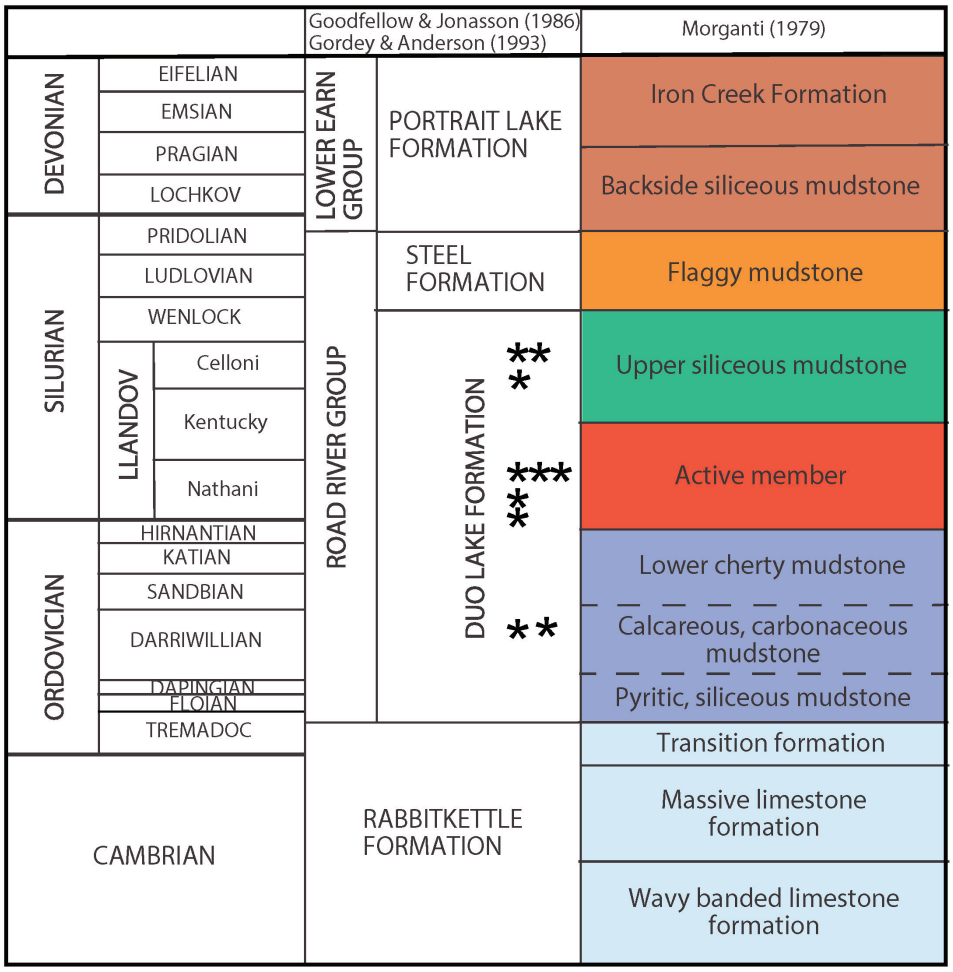

Figure 2. Stratigraphic section of the Howard's Pass district, Yukon. The Zn-Pb mineralization is hosted entirely within the Active member of the Duo Lake Formation (*modified from* Gadd et al. (2016) and Gordey and Anderson (1993)). The asterisks denote the approximate stratigraphic positions of the samples we studied.

The Pyritic Siliceous Mudstone member (2–10 m thick) is the basal unit of the Duo Lake Formation in the Howard's Pass district and consists of grey to black pyritic, carbonaceous shale. The Calcareous Carbonaceous Mudstone member (50–100 m thick) overlies the Pyritic Siliceous Mudstone member and consists of highly carbonaceous mudstone with variable amounts of intercalated limestone and carbonate concretions. Minor wispy pyrite and calcite veins, 2.5 mm to 1 cm wide, occur locally. The Lower Cherty Mudstone Member (15–30 m thick) consists of highly carbonaceous and siliceous mudstone. The Calcareous Carbonaceous Mudstone and Lower Cherty Mudstone members are similarly massive and monotonous, highly carbonaceous cherty mudstones with variable contents of calcite and silica; however, the latter is more siliceous. The Active member (0–60 m thick, and typically 20–30 m) hosts the Zn-Pb mineralization in the Howard's Pass district. Conodonts recovered from the Active member place the time of formation in the lower to middle Llandovery (443–439 Ma; Norford and Orchard, 1985; Kelley et al., 2017). The Upper Siliceous Mudstone member (20–90 m thick) consists of carbonaceous and cherty mudstones with minor to abundant laminations (0.5–1.5 cm thick) of carbonate-rich fluorapatite and locally abundant carbonate concretions. Pyrite is a widespread but minor constituent in all of the members.

Mineralization in the Howard's Pass district occurs along what is termed the Zinc Corridor, a 38 km long, northwest-trending series of 14 SEDEX Pb-Zn deposits that together contain an estimated 400 700 000 t grading 4.5% Zn and 1.5% Pb (Kirkham et al., 2012). These deposits are all located along the same 20 to 30 m thick Llandovery-aged interval, which is composed dominantly of massive and semi-massive sphalerite and galena hosted in calcareous and cherty mudstones; pyrite is a minor component of the mineralization. The XY Central deposit has an indicated resource of 44 450 000 t grading 6.17 weight per cent Zn and 2.64 weight per cent Pb and an inferred resource of 45 940 000 t grading 4.20 weight per cent Zn and 1.32 weight per cent Pb (Kirkham et al., 2012). The XY Central deposit has a strike length of 2.5 km and is interpreted to be on the south limb of a large regional syncline (Yukon Geological Survey, 2020) formed during the Cordilleran Orogeny (Martel, 2015).

Richardson trough and HEBS deposits

The northern Yukon HEBS showings are located within Paleozoic basinal strata of the Richardson trough (Fig. 1). This tectonic depression has been interpreted as a Paleozoic failed rift (Pugh, 1983; Norris, 1985) formed by back-arc extension or compression (Fraser and Hutchison, 2017). It is bounded to the east by the Mackenzie platform and to the west by the Yukon block, the latter of which was a stable, offshore shelf during the pre-Carboniferous Paleozoic (Fig. 1; Morrow, 1999; Strauss et al., 2020). Sedimentary strata within the Richardson trough are characterized by greater than 1000 m of fine-grained, carbonaceous, siliciclastic rocks of the upper Cambrian to Middle Devonian Road River Group (Fig. 3a; Morrow 1999). The Imperial Formation is correlative to the Earn Group strata in the Howard's Pass district to the southeast (Gordey, 2008). The Canol Formation conformably overlies the Road River Group and consists of as much as 220 m of Middle Devonian to lower Upper Devonian cherty, carbonaceous shale (Fraser and Hutchison, 2017). The terminal Road River Group is a regionally extensive condensed section (Fraser and Hutchison, 2017; Gadd and Peter, 2018).

A thin (1–10 cm thick) HEBS layer is documented at the Canol Formation–Road River Group contact in several localities throughout northern Yukon, including at Peel River and Nick. The HEBS layers consist of approximately 60 volume per cent sulfide minerals (pyrite, millerite, vaesite, and sphalerite) and 40 volume per cent non-sulfide minerals (Hulbert et al., 1992; Gadd et al., 2019); the sulfide minerals are interbedded with black, siliceous shale. Samples typically display sedimentary features that include laminar bedding disrupted by soft-sediment deformation. The upper and lower contacts with the enclosing host rocks are typically sharp, but minor slumping into the underlying siliceous shales may be locally present. Minor to abundant biogenic debris is present and includes conodont elements and pyrite-permineralized plant matter (Gadd and Peter, 2018). There is a low abundance of terrigenous clastic detritus (Gadd, Peter, and Layton-Matthews, this volume).

The stratigraphic sections of the Peel River showing (Fig. 3b) and the Nick prospect (Fig. 3c) are lithologically similar, with local variations in the thicknesses of units. The rock types include 1) black shale with 0.5 to 1.5 m diameter calcareous concretions; 2) siliceous black shale with minor calcareous intercalations; 3) a 1 to 10 cm thick stratiform semi-massive Ni–Zn–Fe-sulfide HEBS layer; and 4) siliceous to cherty black shale that is in sharp contact with the underlying HEBS mineralization. A significant difference between the stratigraphic sections of the two locations is that three distinct HEBS layers have been documented at Peel River (Gadd et al., 2019), whereas only one is identified at the Nick prospect (cf. Fig. 3b, c). Gadd, Peter, and Layton-Matthews (this volume) present a synopsis of the geological, geochemical, and geochronological characteristics of HEBS in the northern Canadian Cordillera, including the Peel River and Nick deposits.

SAMPLING

At each of the three localities, we selected samples that are representative of mineralized strata and unmineralized shale and mudstone from the immediate stratigraphic footwall and hanging wall, plus one sample of an approximately 2 m wide pyrobitumen vein at the Nick deposit. Sample descriptions and metadata are given in Table 1.

All outcrop samples were collected using a standard geological pick and chisel and stored in polyethylene sample bags. Samples could not be collected from outcrop at XY Central given the extreme weathering and oxidation of the surfaces; therefore, samples of this deposit were collected from the ore pile and drill core (hole XYC-224). Some drill core samples from XY Central may have had vestigial traces of wax crayon markings made during the course of drill core logging; however, we made every effort to avoid sampling drill core with such markings and, for those samples where it could not be avoided, we removed all visible evidence of the wax by vigorously wire-brushing the core surface. The samples were stored in polyethylene sample bags.

METHODOLOGIES

Rock-Eval analysis

Rock-Eval pyrolysis is used to identify the type and maturity of organic matter and to detect petroleum potential in sediments and sedimentary rocks (e.g. Tissot and Welte, 1984; Espitalié, 1986; Behar et al., 2001). During Rock-Eval pyrolysis, a small sample is heated (in a pyrolysis oven) to programmed temperatures in an inert atmosphere to quantitatively and selectively determine 1) the free hydrocarbons contained in the sample and 2) the hydrocarbon- and O-containing compounds (e.g. CO_2) volatilized during the cracking of the unextractable organic matter (kerogen) in the sample.

Rock-Eval and TOC analyses of rock samples were performed at the Geological Survey of Canada (GSC) laboratories (Calgary, Alberta) on a Wildcat Technologies HAWK (hydrocarbon analyzer with kinetics) pyrolysis and TOC instrument with dual pyrolysis and combustion functions. Details of the analytical procedure are presented in Jiang et al. (2017). Briefly, thermal desorption was conducted at 300°C for 3 min to produce the S1 peaks and then pyrolysis was conducted from 300 to 650°C at a temperature increase of 25°C/min to yield the S2 hydrocarbon peaks and S3 CO and CO_2 peaks as parts of productive organic carbon (PC) and pyrolysis mineral carbon. Combustion was then performed from 300 to 850°C to determine the residual organic carbon (RC) and oxidation mineral carbon from CO and CO_2 generated during oxidation. The following parameters were measured during pyrolysis:

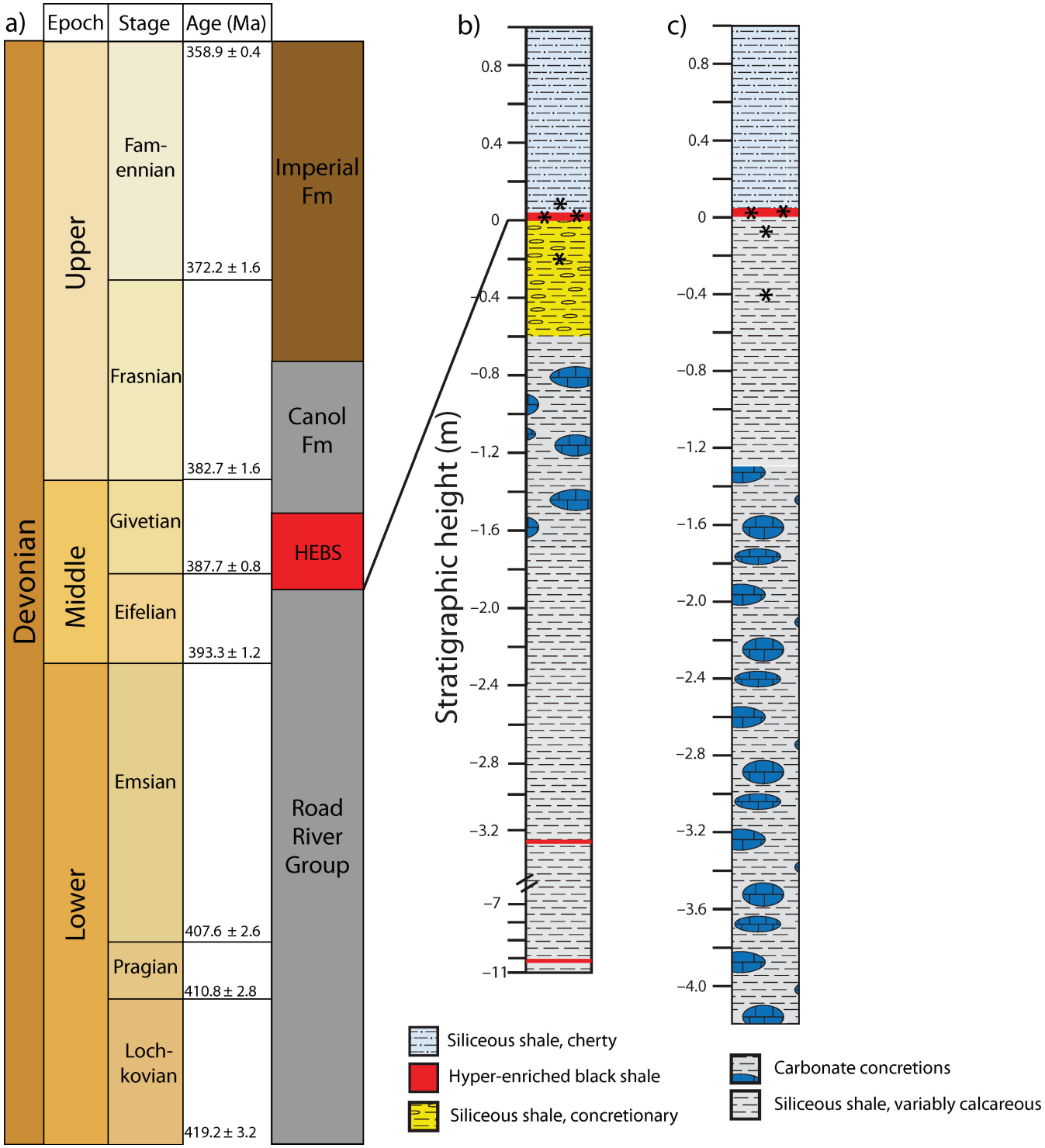

Figure 3. a) Devonian stratigraphy of the Richardson trough, northern Yukon, with schematic stratigraphic sections that highlight the lithostratigraphy at the **b)** Peel River and **c)** Nick hyper-enriched black shale (HEBS) localities. The '0' mark is positioned at the base of the HEBS layer, which occurs at the stratigraphic contact between the Road River Group and the Canol Formation (*modified from* Gadd, Peter, and Layton-Matthews, this volume). The ages are based on the Devonian time scale of Becker et al. (2012). The asterisks denote the stratigraphic positions of the samples we studied (one sample of a pyrobitumen vein at the Nick locality, located tens to hundreds of metres below the HEBS layer is not shown (off the scale of the figure).

Table 1. Sample descriptions and metadata for shale samples from the XY Central sedimentary exhalative (SEDEX) deposit (Howard's Pass district) and Peel River and Nick hyper-enriched black shale (HEBS) deposits (Richardson trough), Yukon.

Lab ID	Sample ID	Sample number	Locality	Sub-location	Description	Sample type	Depth (m)
HYPER-ENRICHED BLACK SHALE DEPOSIT							
X12068	O-256540	17-POA-056	Peel River	North bank	Fissile, carbonaceous shale 20 cm below HEBS mineralization	Riverbank outcrop	NA
X12069	O-256541	17-POA-300	Peel River	North bank	Cherty, carbonaceous shale of Canol Formation 5 cm above HEBS mineralization	Riverbank outcrop	NA
X12070	O-256542	17-POA-301	Peel River	North bank	HEBS (Ni-Mo-Zn-PGE-Au-Re) with pyrite permineralized terrestrial plant remains	Riverbank outcrop	NA
X12071	O-256543	17-POA-302	Peel River	North bank	HEBS (Ni-Mo-Zn-PGE-Au-Re) with visible conodonts	Riverbank outcrop	NA
X12072	O-256544	18-POA-078	Nick property	Discovery showing	Carbonaceous shale 10 cm below HEBS mineralization	Creek outcrop	NA
X12073	O-256545	18-POA-081	Nick property	Discovery showing	Carbonaceous shale 40 cm below HEBS mineralization	Creek outcrop	NA
X12074	O-256546	18-POA-123	Nick property	Mawer Falls	HEBS (Ni-Mo-Zn-PGE-Au-Re)	Creek outcrop	NA
X12075	O-256547	18-POA-125	Nick property	Gorge showing	HEBS (Ni-Mo-Zn-PGE-Au-Re)	Creek outcrop	NA
X12076	O-256548	18-POA-131	Nick property	Pyrobitumen vein	Conchoidally fracturing, lustrous pyrobitumen vein (≈ 2–3 m wide) crosscutting limestone; tens to hundreds of metres below HEBS	Creek outcrop	NA
SEDEX DEPOSIT							
X12077	O-256549	11-POA-001	Howard's Pass	XY Central	Active member, mineralized (highly sheared semimassive sphalerite, galena in calcareous matrix) shale	Ore pile specimen	NA

Contents

Table 1. (cont.) Sample descriptions and metadata for shale samples from the XY Central sedimentary exhalative (SEDEX) deposit (Howard's Pass district) and Peel River and Nick hyper-enriched black shale (HEBS) deposits (Richardson trough), Yukon.

Lab ID	Sample ID	Sample number	Locality	Sub-location	Description	Sample type	Depth (m)
X12078	O-256550	11-POA-002	Howard's Pass	XY Central	Active member, mineralized (laminated semi-massive sphalerite, pyrite, galena) shale; minor sulfide remobilization into cleavages	Ore pile specimen	NA
X12079	O-256551	11-POA-003	Howard's Pass	XY Central	Active member, mineralized (sphalerite laminae intercalated with laminated carbonaceous mudstone); dewatering structures evident	Ore pile specimen	NA
X12080	O-256552	XYC-224;87.1	Howard's Pass	XY Central	Upper siliceous mudstone, massive, black, minor pyrite; close to FLMD/USMS contact	Drill core	87.1
X12081	O-256553	XYC-224;88.5	Howard's Pass	XY Central	Upper siliceous mudstone, massive, black, calcareous mudstone with abundant pyrite framboids	Drill core	88.5
X12082	O-256554	XYC-224;116.8	Howard's Pass	XY Central	Upper siliceous mudstone, banded, black, with carbonate-, phosphate-, and pyrite-rich bands	Drill core	116.8
X12083	O-256555	XYC-224;155.9	Howard's Pass	XY Central	Upper siliceous mudstone, light grey with carbonate concretion	Drill core	155.9
X12084	O-256556	XYC-224;167.3	Howard's Pass	XY Central	Active member, unmineralized, laminated, dark grey shale	Drill core	166.4
X12085	O-256557	XYC-224;196.2	Howard's Pass	XY Central	Active member, unmineralized, laminated, dark grey shale with minor framboidal pyrite	Drill core	196.2
X12086	O-256558	XYC-224;202.0	Howard's Pass	XY Central	Calcareous, carbonaceous mudstone, medium grey, bedded, minor carbonate concretions, abundant fine-grained pyrite	Drill core	202.0
X12087	O-256559	XYC-224;205.1	Howard's Pass	XY Central	Calcareous, carbonaceous mudstone, black, with minor framboidal pyrite	Drill core	205.1

HEBS: hyper-enriched black shale; FLMD: flaggy mudstone; NA: not applicable; USMS: Upper siliceous mudstone

- S1 (free hydrocarbon yield) – the amount of volatile hydrocarbons (gas and oil) in the sample, measured in milligrams of hydrocarbon (HC) per gram of rock. S1 is measured during the initial 300°C heating step of pyrolysis.
- S2 (potential hydrocarbon yield) – the amount of hydrocarbons generated through thermal cracking of non-volatile organic matter (in mg HC/g rock). S2 is an indication of the quantity of hydrocarbons that the rock has the potential to produce if burial and maturation continues. This parameter is measured during the ramped heating stage, from 300 to 650°C.
- S3 (organic CO and CO_2 yield) – the amount of CO and CO_2 (in mg CO_2/g rock) produced during the pyrolysis of kerogen at temperatures below 390°C. S3 is a measure of the organic CO and CO_2 yield of the rock, which is an indication of the amount of O in the kerogen, and is used to calculate the oxygen index (OI; *see* below). Contamination of the samples should be suspected if abnormally high S3 values are obtained. High concentrations of carbonate minerals that break down at temperatures below 390°C will also cause higher than expected S3 values.
- S4 – the amount of CO_2 (in mg CO_2/g rock) produced from the organic residue remaining after the pyrolysis of kerogen is completed; this is used to determine the RC value.
- T_{max} (thermal maturity) – the temperature (in °C) at which the maximum release of hydrocarbons from kerogen cracking occurs during pyrolysis. T_{max} corresponds to the temperature at the top of the S2 peak and serves as a measurement of thermal maturity (a stage of maturation) of the organic matter (Behar et al., 2001). T_{max} is only reliable if S2 >0.2 mg HC/g rock (Peters, 1986).

Additional parameters are derived from these measurements:

- TOC – the total organic carbon (TOC) content is the sum of the pyrolyzable organic carbon (PC) and residual organic carbon (RC) in weight per cent. The PC represents the present-day generative organic carbon, whereas the RC represents the present day non-generative part of the organic carbon in the sample.
- MinC – the mineral carbon (MinC; also called carbonate carbon, CC) is the sum of the pyrolysis mineral carbon and oxidation mineral carbon and is indicative of the carbonate mineral content of the rock (in weight per cent).
- HI – the hydrogen index represents the amount of potential hydrocarbons relative to the amount of total organic carbon: HI= S2/TOC × 100.
- PI – the production index represents the amount of free hydrocarbons relative to the amount of organic matter in the rock, and is determined by S1/(S1+S2).
- OI – the oxygen index represents the amount of organic-bound O relative to the amount of organic C present in a sample: OI = S3/TOC × 100.

Organic petrography

Organic petrography can provide information about the source-rock type and associated organic matter, thermal maturity, and hydrocarbon generation zone (e.g. Taylor et al., 1998). Kerogens have a high molecular weight relative to bitumen or SOM. Bitumen forms from kerogen during petroleum generation. Typical organic constituents of kerogen are algae and woody plant material. Kerogens are described as: type I, consisting of mainly algal and amorphous (algal and bacterial remains) kerogen and highly likely to generate oil; type II, mixed terrestrial- and marine-sourced material that can generate waxy oil; or type III, woody terrestrial source material that typically generates gas (e.g. Tissot and Welte, 1984).

Macerals are organic components of a rock that are analogous to the minerals in rocks. Maceral analysis provides a detailed composition of organic matter types present. Major maceral groups are liptinite, vitrinite, and inertinite (e.g., Taylor et al., 1998). The liptinite group is further divided into alginite (preserved algal remains), bituminite, and other oil-prone macerals, such as sporinite from land plant spores and liptodetrinite, which is a collection of small liptinite fragments (Kus et al., 2017; Pickel et al. 2017). Bituminite (i.e. amorphous organic matter) is an insoluble maceral that has undergone bacterial, thermal, and physicochemical degradation, and occurs as layers or intermixed with mineral matter (Kus et al., 2017). Solid bitumen is a product of organic matter transformation and thermal cracking of produced oil. It fills intergranular pore spaces and cracks. It is a solid residue that remains in the source rock after thermal cracking and oil migration. Bitumen can convert to pyrobitumen at high temperatures; this is characteristic of oil-to-gas cracking (Curiale, 1986; Jacob, 1989).

Interpretations of thermal maturity and the hydrocarbon generation zone are based on the reflectance measurements and overall observations of organic matter under the microscope with white and ultraviolet light in oil immersion or dry environment. Data recorded include vitrinite reflectance and solid bitumen reflectance.

Maceral observations and reflectance measurements were performed at the GSC laboratories (Calgary, Alberta) on polished pellets, constructed by mounting mixtures of rock chips and resin in plastic molds, using a Zeiss Axioplan microscope equipped with an ultraviolet source and Hilgers DISKUS-FOSSIL software. Classification of the main groups of dispersed organic matter is reported according to

the International Committee for Coal and Organic Petrology (ICCP) official classification (ICCP, 1993; Kus et al., 2017; Pickel et al. 2017). Fluorescence microscopy was carried out using ultraviolet G 365 nm excitation with a 420 nm barrier filter. The random reflectance measurement was carried out under oil immersion following the ASTM D7708-11 method (ASTM International, 2011). Due to the absence of true vitrinite macerals within the samples (*see* Results), the reflectance of solid pyrobitumen was measured. The reflectance data reported in this paper are measured reflectance of pyrobitumen or solid bitumen. Vitrinite reflectance has also been calculated from these values according to the conversion equation of Schmidt et al. (2019) and reported in Table 2.

Solvent extraction

Prior to GCMS analysis, solvent extraction was conducted at the GSC laboratories (Calgary, Alberta). Approximately 20 to 40 g of each powdered rock sample were subjected to Soxhlet extraction for 72 h using dichloromethane solvent. Activated copper grains were added to the extract at the end of the extraction period or during solvent removal to remove any elemental sulfur. After removing most of the solvent using a rotary evaporator, the extract contents were filtered to remove copper, copper sulfide, and any other solids. The amount of extract (<3 mg) from each sample in this study was insufficient for saturate-aromatics-resin-asphaltene separation (SARA: saturates contain only single bonds between carbon atoms; aromatics have sigma bonds and delocalized pi electrons between carbon atoms forming a circle; resins are highly viscous polymers; and asphaltenes are the n-alkane insoluble/toluene-soluble fraction). Before complete solvent removal, the extracts were directly analyzed by full-scan GCMS analysis to investigate the molecular compositions of the soluble organic matter (SOM) in the samples. The SOM yields were determined after GCMS analysis and complete solvent removal.

Full-scan GCMS analysis of whole extracts

The very low solvent extraction SOM yields were insufficient for separation into saturated and aromatic fractions for GCMS analysis. For this reason, the SOM was analyzed directly by full-scan GCMS analysis to extract as much meaningful fossil molecular information as possible. The GCMS analysis of the whole solvent extracts was performed at the GSC laboratories (Calgary, Alberta) on an Agilent 6890 series gas chromatograph (GC) coupled to an Agilent 5973 series mass selective detector (MSD) operated in full-scan mode. Split injection was employed using an Agilent J&W DB-5 30 m × 0.32 mm × 0.25 µm capillary column at 300°C with helium carrier gas at a flow rate of 1.2 mL/min. The GC oven temperature was programmed to increase from 40 to 325°C at a rate of 4°C/min and then held for 15 min. Compound identification was based on comparison of GC retention times and mass spectra with those reported in literature and historical data in the GSC organic geochemistry laboratories in Calgary.

RESULTS

Bulk organic property by Rock-Eval analysis

Rock-Eval analysis indicates that all shale samples from XY Central, Peel River, and Nick are rich in organic matter (Table 2): XY Central: TOC = 1.50 to 11.39 (mean 6.25) weight per cent; Peel River: TOC = 0.33 to 1.86 (mean 1.21) weight per cent; and Nick: TOC = 1.93 to 4.60 (mean 3.34) weight per cent. The Nick pyrobitumen sample has a much higher TOC content (65.45 weight per cent).

Although the samples have high organic carbon contents, their S1 values, representing the amount of free hydrocarbons currently present in the rock samples, are very low (Table 2): XY Central: S1 = 0 to 0.09 (mean 0.04) mg HC/g rock; Peel River: S1 = 0.08 to 0.11 (mean 0.10) mg HC/g rock; and Nick: S1 = 0.07 to 0.08 (mean 0.08) mg HC/g rock. In contrast, the Nick pyrobitumen sample has a lower S1value (0.02 mg HC/g rock) than the other shale and HEBS samples.

Concomitantly, S2 values, representing the potential for hydrocarbons to be generated upon further thermal maturation, are also very low (Table 2): XY Central: S2 = 0 to 0.22 (mean 0.12) mg HC/g rock; Peel River: S2 = 0.18 to 0.23 (mean 0.20) mg HC/g rock; and Nick: S2 = 0.17 to 0.18 (mean 0.18) mg HC/g rock. In contrast, the Nick pyrobitumen sample has a lower S2 value (0.11 mg HC/g rock) than the other shale and HEBS samples. Hydrogen index values are also very low (mostly below 20; Table 2): XY Central: HI = 0 to 5 (mean 2.27) mg HC/g TOC; Peel River: HI = 11 to 53 (mean 24) mg HC/g TOC; and Nick: HI = 3 to 8 (mean 5) mg HC/g TOC. In contrast, the Nick pyrobitumen sample has a lower HI value (0 mg HC/g TOC) than the other shale and HEBS samples.

Residual organic carbon values are (Table 2): XY Central: RC = 98.0 to 99.6 (mean 99.1) weight per cent of TOC; Peel River: RC = 84.8 to 96.8 (mean 93.2) weight per cent of TOC; and Nick: RC = 97.4 to 99.1 (mean 98.2) weight per cent of TOC. In contrast, the Nick pyrobitumen sample has an RC value (99.9 weight per cent of TOC) that is higher than the other shale and HEBS samples.

Values of T_{max}, an indicator of thermal maturity, are (Table 2): XY Central: T_{max} = 322 to 438°C (mean 372°C); Peel River: T_{max} = 446 to 599°C (mean 498°C); and Nick: T_{max} = 338 to 415°C (mean 380°C). The Nick pyrobitumen sample has a T_{max} value (395°C) that is within the range measured for the shale and HEBS samples.

Table 2. Solvent extraction yields and Rock-Eval, pyrobitumen reflectance, and vitrinite reflectance data for shale samples from the XY Central sedimentary exhalative (SEDEX) deposit (Howard's Pass district) and Peel River and Nick hyper-enriched black shale (HEBS) deposits (Richardson trough), Yukon. Vitrinite reflectance values calculated from pyrobitumen reflectance using the equation of Schmidt et al. (2019).

Lab ID	Solvent extraction yield (mg/g rock)	S1 (mg (HC/g rock)	S2 (mg (HC/g rock)	HI (mg HC/g TOC)	OI (mg CO_2/g TOC)	T_{max} (°C)	TOC (wt %)	RC (wt %)	MinC (wt %)	Pyrobitumen reflectance (%)	SD	N	Vitrinite equivalent reflectance (%)
HYPER-ENRICHED BLACK SHALE DEPOSIT													
X12068	0.05	0.09	0.21	11	11	476	1.86	96.80	0.12	1.83	0.01	43	2.03
X12069	0.04	0.11	0.23	18	13	599	1.30	96.20	0.07	1.75	0.11	46	1.96
X12070	0.02	0.10	0.18	13	24	470	1.35	94.80	0.18	1.89	0.19	42	2.09
X12071	0.01	0.08	0.18	53	90	446	0.33	84.80	1.07	2.13	0.46	36	2.31
Mean	0.03	0.10	0.20	24	35	498	1.21	93.15	0.36	1.90	0.19	42	2.10
X12072	0.01	0.08	0.17	8	14	338	1.93	97.40	2.51	3.84	0.48	61	3.92
X12073	0.02	0.07	0.18	3	9	415	4.60	99.10	0.06	4.05	0.78	52	4.11
X12074	0.00	0.08	0.17	5	11	369	2.90	97.90	0.08	4.05	0.78	52	4.11
X12075	0.01	0.08	0.18	4	15	399	3.93	98.20	0.16	4.53	0.71	71	4.56
Mean (excluding pyrobitumen vein)	0.01	0.08	0.18	5.00	12.25	380	3.34	98.15	0.70	4.12	0.69	59	4.18
X12076	0.06	0.02	0.11	0	1	395	65.45	99.90	3.88	5.64	0.4	60	5.60
SEDEX DEPOSIT													
X12077	0.01	0.05	0.09	5	21	385	1.50	98.00	2.74	20.83*	0.57	58	19.85*
X12078	0.15	0.05	0.15	2	6	361	5.70	99.30	2.64	5.60	1.27	50	5.57
X12079	0.04	0.09	0.17	4	14	358	3.78	98.40	2.57	5.30	1.52	69	5.29
X12080	0.08	0.03	0.12	1	4	369	8.02	99.50	0.59	4.99	0.89	81	5.00
X12081	0.04	0.04	0.13	2	6	358	6.51	99.40	4.74	5.45	0.91	76	5.43
X12082	0.06	0.03	0.12	1	3	376	8.74	99.50	0.76	5.00	0.64	71	5.00
X12083	0.07	0.04	0.11	1	4	338	8.47	99.60	1.39	5.52	1.05	88	5.49
X12084	0.06	0.04	0.14	3	13	438	3.51	98.90	2.73	5.02	1.28	80	5.02
X12085	0.05	0.00	0.00	0	5	399	11.39	99.50	0.51	5.48	1.08	86	5.45
X12086	0.07	0.07	0.22	5	15	385	3.78	98.40	7.96	5.15	0.72	73	5.15
X12087	0.04	0.04	0.09	1	7	322	7.39	99.5	0.15	5.80	1.11	84	5.75
Mean	0.06	0.04	0.12	2.27	8.91	372	6.25	99.09	2.43	5.33	1.00	74	5.31

HC: hydrocarbon; HI: hydrogen index; MinC: mineral carbon; OI: oxygen index; RC: residual organic carbon; S1: free hydrocarbon in sample; T_{max}: temperature of maximum release of hydrocarbons; TOC: total organic carbon before analysis; S2 = volume of hydrocarbon released during analysis; Refl. = Reflectance; SD = Standard deviation; N = number of measurements
*outlier; not used for calculation of mean value

Bulk organic property by petrographic observation

The organic macerals of the studied samples are dominated by over-mature granular amorphous kerogen that has been exhausted of hydrocarbon elements. Trace amounts of granular pyrobitumen, both isotropic and anisotropic, are also present in all shale samples. Pyrobitumen reflectance values (R_o) are: XY Central: 4.99 to 5.80% (mean 5.33%) ; Peel River: 1.75 to 2.13% (mean 1.90%); and Nick: 3.84 to 4.53% (mean 4.12%) (Table 2). In contrast, the Nick pyrobitumen sample has a reflectance value (5.64%) that is somewhat higher than the range for the shale and HEBS samples. One sample from XY Central generated an R_o reading of 20.83%, which is well outside of the range of the other samples. This outlier value may have been measured from pyrite, and is therefore omitted from further consideration and statistics.

Molecular signatures by GCMS analysis of solvent extracts

Solvent extraction of the samples produced very low amounts of SOM, mostly less than 0.08 mg/g rock (Table 2): XY Central: 0.01 to 0.15 (mean 0.06) mg/g rock; Peel River: 0.01 to 0.05 (mean 0.03) mg/g rock; and Nick: 0 to 0.02 (mean 0.01) mg/g rock. In contrast, the Nick pyrobitumen sample had a solvent extraction yield (0.06 mg/g rock) that is somewhat higher than the range for the shale and HEBS samples.

Figures 4, 5, 6, and 7 present the total ion chromatograms (TICs) from GCMS analysis of the SOM extracted from Peel River, Nick and the XY Central samples. Elemental sulfur was detected by GCMS analysis in certain samples (peaks labelled S8 in Fig. 4, 5, 6).

Figure 8 presents mass chromatograms showing detailed distributions of naphthalenes (the simplest polycyclic aromatic hydrocarbons (PAHs), a group of aromatic hydrocarbons containing two or more fused benzene rings) and dibenzothiophenes (organosulfur compounds consisting of two benzene rings fused to a central thiophene ring). Figure 9 shows the detection of biphenyls (aromatic hydrocarbon with a molecular formula $(C_6H_5)_2$) and phenanthrenes (PAHs composed of three fused benzene rings), and Figure 10 displays the distributions of diamondoid compounds, a class of very thermally stable hydrocarbons.

DISCUSSION

Thermal maturity

The thermal maturity of organic matter is typically assessed using R_o, determined from organic petrography, and T_{max}, from Rock-Eval pyrolysis (Espitalié, 1986; Peters and Cassa, 1994). The Rock-Eval pyrograms (not shown) for all samples exhibit extremely low, flat S2 peaks; therefore, all T_{max} values (below 476°C) except one outlier at Peel River (599°C) are considered to be unreliable and not indicative of the samples' true thermal maturity. Wide, flat S2 peaks with very low S2 values (<0.23 mg HC/g rock) occur mostly in over-mature source rocks (Peters, 1986; Riediger et al., 2004; Obermajer et al., 2007). The organic carbon contained in the shale, mudstone, and pyrobitumen (>98 weight per cent) is mainly 'dead' organic carbon or RC that has been exhausted of hydrocarbon generation potential due to extreme thermal exposure. Nevertheless, the slightly but consistently higher HI values and lower percentage of RC measured in Peel River samples compared to those from Nick and XY Central (Table 2) indicate that the Peel River strata have experienced somewhat lower temperatures than those at Nick and in the Howard's Pass district. Further evidence of this comes from pyrobitumen reflectance values at Peel River (1.75–2.13%), which are lower than those at Nick (3.84–4.53%) and XY Central (4.99–20.83%; Table 2).

The very low solvent extraction yields (Table 2) are broadly reflective of the Rock-Eval S1 values, which indicate the presence of thermally desorbed hydrocarbons, further indicating that the shale, mudstone, and pyrobitumen samples now contain only trace liquid hydrocarbons.

Steranes (a class of tetracyclic compounds derived from steroids or sterols) and tricyclic and pentacyclic terpanes (C_{19}–C_{45}) have been widely used to infer organic input, depositional environment, and thermal maturity of crude oils and their source rocks in the oil and wet gas windows (Peters et al., 2005); however, these polycyclic alkanes are thermally unstable and are readily broken down to light hydrocarbons at elevated temperatures, leading to reduced concentrations in the condensate window and disappearance in the dry gas window (Dahl et al., 1999; Peters et al., 2005). These biomarkers were not detected in any of the samples studied, which is consistent with thermal maturity levels beyond the oil window and into the dry gas window, as indicated by Rock-Eval analysis and petrographic observation. Likewise, porphyrins, a class of metal-containing biomarkers specific to immature to low-maturity sediments (Peters et al., 2005), do not appear to be present in the studied shale samples either based on the colorless nature of the solvent extracts.

Similar to saturated hydrocarbons, PAHs that occur widely in crude oils and source rocks in the oil and wet gas windows were not detected in the SOM of samples from Nick and XY Central. In contrast, PAHs with two to five rings are present as the main GC-amenable components of the Peel River samples; these include naphthalenes, biphenyls, phenanthrenes, benzofluoranthenes, and benzopyrenes (Fig. 4). The parental PAHs mostly dominate over their alkylated derivatives (with one to a few methyl groups), also indicating the high thermal maturity of the shales.

The high thermal maturity of the Peel River shales is also evident from the isomer distributions of the alkyl PAHs, such as the dominance of 3- and 2- over 9- and 1-methylphenathrens (Fig. 9), and 4- over 1-methyldibenzothiophene (Fig. 8);

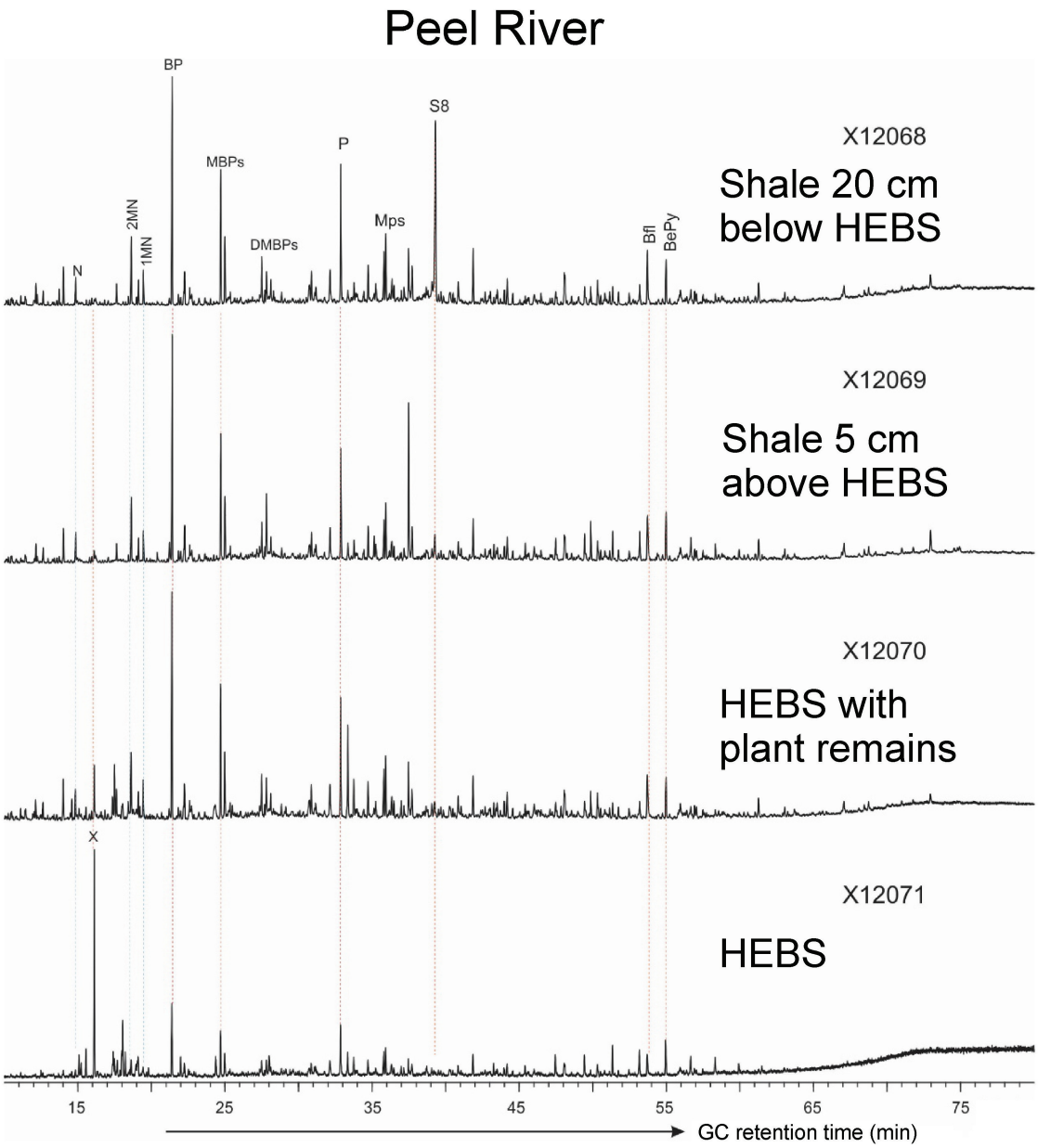

Figure 4. Total ion chromatograms from full-scan gas chromatography mass spectrometry analyses showing the composition of soluble organic matter in shale samples (X12068–X12071) from the north bank of the Peel River deposit, Richardson trough, Yukon. Abbreviations: 1MN: 1-methyl naphthalene; 2MN: 2- methyl naphthalene; BePy: benzo(e)pyrene; Bfl: benzofluoranthene; BP: biphenyl; DMBPs: dimethyl biphenyls; HEBS: hyper-enriched black shale; MBPs: methyl biphenyls; MPs: methyl phenanthrenes; N: naphthalene; P: phenanthrene; S8: elemental sulfur; X: unknown compound, likely a contaminant.

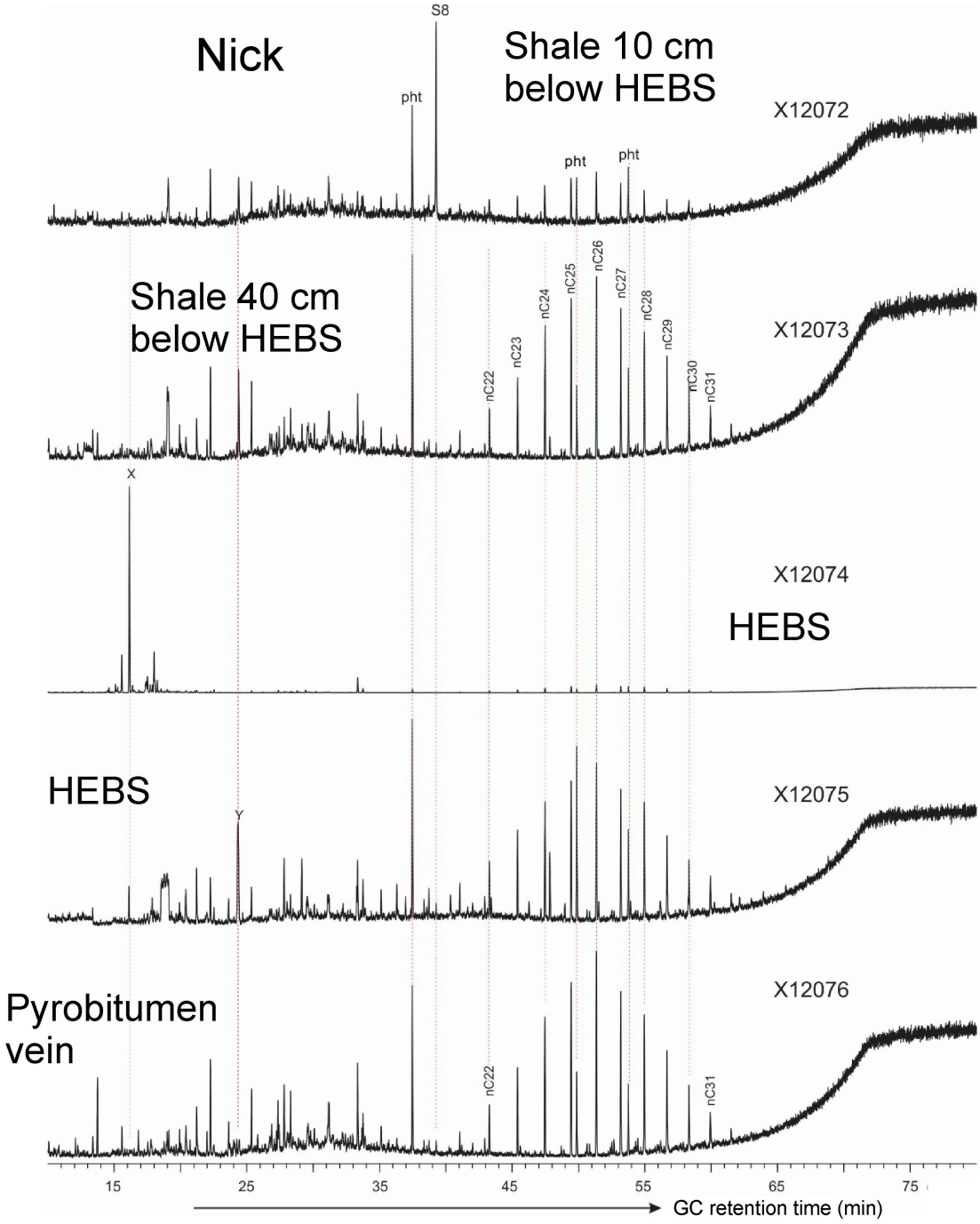

Figure 5. Total ion chromatograms from full-scan gas chromatography mass spectrometry analyses showing the composition of soluble organic matter in shale samples (X12072–X12076) from the Nick property, Richardson trough, Yukon. Abbreviations: HEBS: hyper-enriched black shale; nC22 to nC31: corresponding *n*-alkanes, likely contaminants from wax-containing materials; pht: plasticizers; S8: elemental sulfur; X, Y: unknown compounds, likely contaminants.

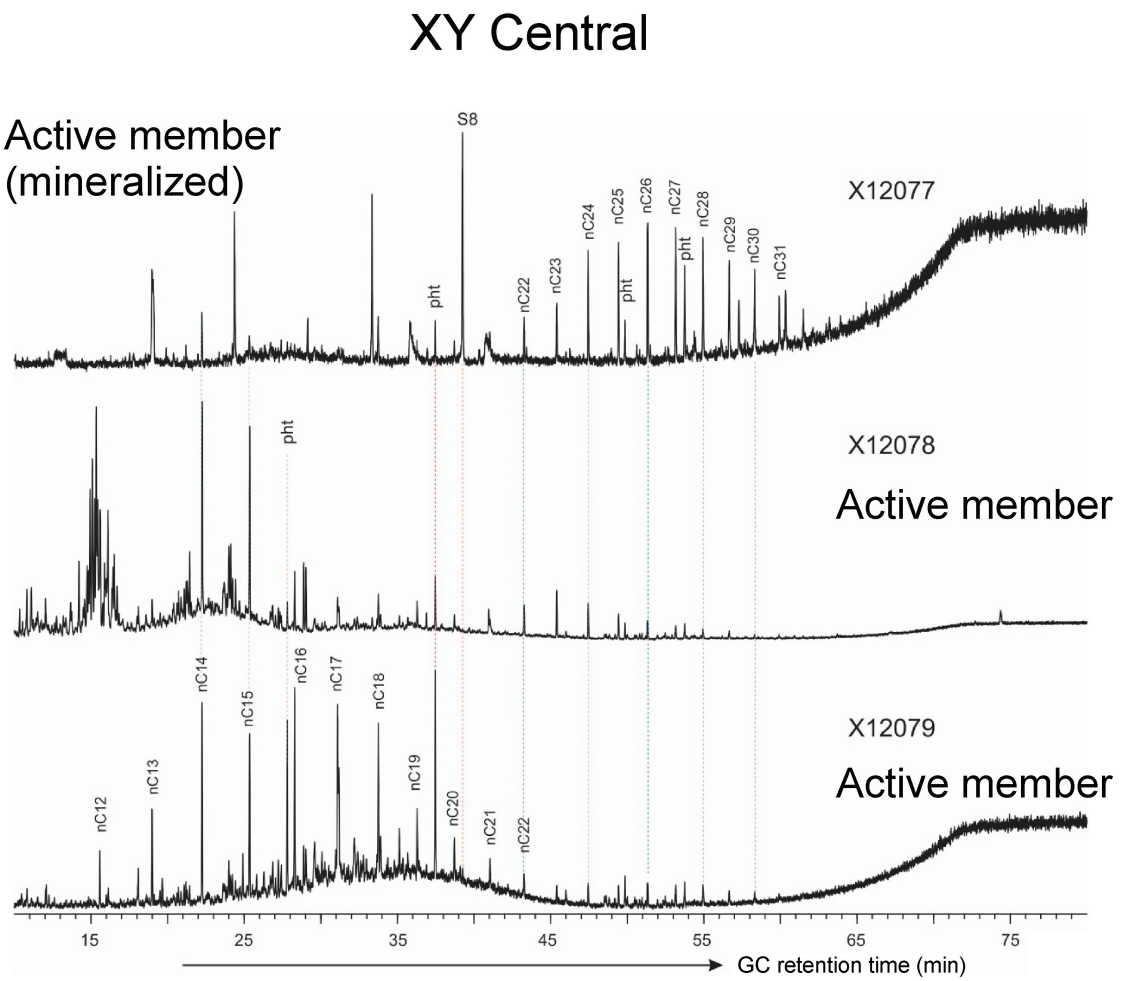

Figure 6. Total ion chromatograms from full-scan gas chromatography mass spectrometry analyses showing the composition of soluble organic matter in surface shale samples (X12077–X12079) from the XY Central ore pile, Howard's Pass district, Yukon. Abbreviations: 1MN: 1-methyl naphthalene; 2MN: 2- methyl naphthalene; nC12 to nC31: corresponding **n**-alkanes, likely contaminants from wax-containing materials; pht: plasticizers; S8: elemental sulfur.

however, the presence of abundant PAHs at Peel River, together with their paucity at Nick and XY Central, is further evidence that Peel River has experienced less severe heating than the latter two deposits. Although the thermal destruction of the PAHs could perhaps be attributed to the effects of hydrothermal alteration overprint on the mineralizing process in XY Central samples (e.g. Peter et al., 2015), this cannot explain their absence at Nick, which is not thought to have formed by hydrothermal processes, but rather under ambient marine temperatures (*see* Gadd, Peter, and Layton-Matthews, this volume). The preservation of PAHs at Peel River, and their absence (due to destruction) at Nick and XY Central is likely due to primary thermal maturity variations across the greater Selwyn Basin and Richardson trough area. At XY Central, burial depths for the studied samples are thought to be less than 3 km, giving a temperature of only approximately 75 to 90°C, assuming an average geothermal gradient of 25 to 30°C/km (Hyndman, 2010; *see* Riediger et al., 1989); however, higher geothermal gradients have been invoked to explain anomalous paleotemperature regimes to the north and east-northeast of the northern two study sites (e.g. Issler et al., 2005; Gal et al., 2009; Powell et al., 2019).

Adamantanes (three connected cyclohexane rings arranged in an 'armchair' configuration) and diamantanes (cage hydrocarbons with structures similar to a subunit of the diamond lattice) are present in the Peel River samples (Fig. 10), but below detection in the Nick and XY Central samples. Diamondoids (which include adamantanes and diamantanes) are among the most thermally stable hydrocarbons (Dahl et al., 1999; Peters et al., 2005), and their absence in the Nick and XY Central samples also supports the interpretation that the Nick and XY Central strata have undergone slightly greater thermal maturation than Peel River strata.

Riediger et al. (1989) attributed the high degree of thermal maturity (late catagenesis to early metagenesis) in the Howard's Pass district to anomalously high heat flow, as geological evidence only suggests moderate depths of

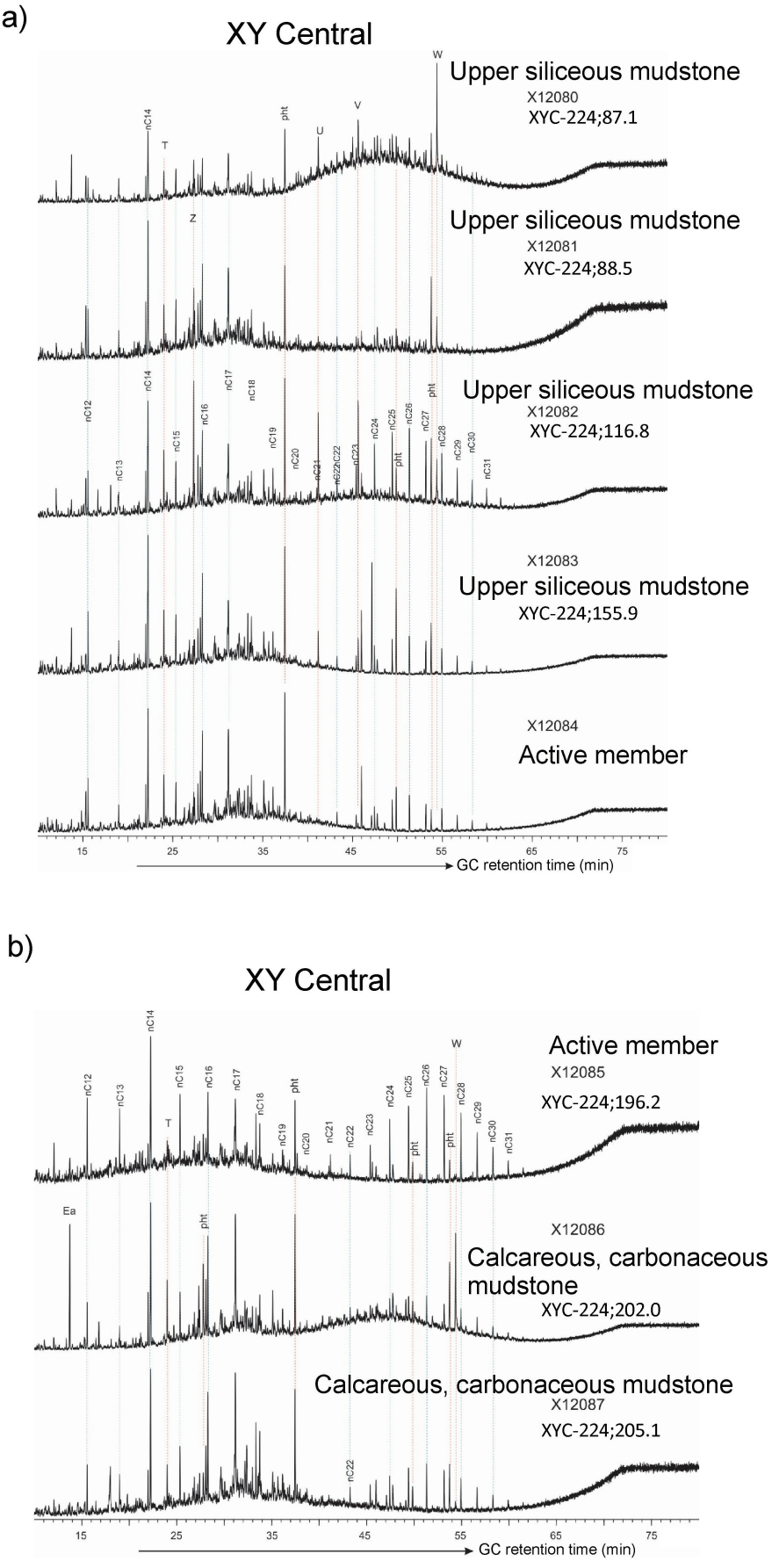

Figure 7. Total ion chromatograms from full-scan gas chromatography mass spectrometry analyses showing the composition of soluble organic matter in **a)** cored shale samples (X12080–X12084) from the XY Central deposit; **b)** cored shale samples (X12085–X12087) from the XY Central deposit, Howard's Pass district, Yukon. Abbreviations: Ea: 2-ethylhexyl acrylate; nC12 to nC31: corresponding n-alkanes, likely contaminants from wax-containing materials; pht: plasticizers; T, U, V, W, and Z: unknown compounds, likely contaminants.

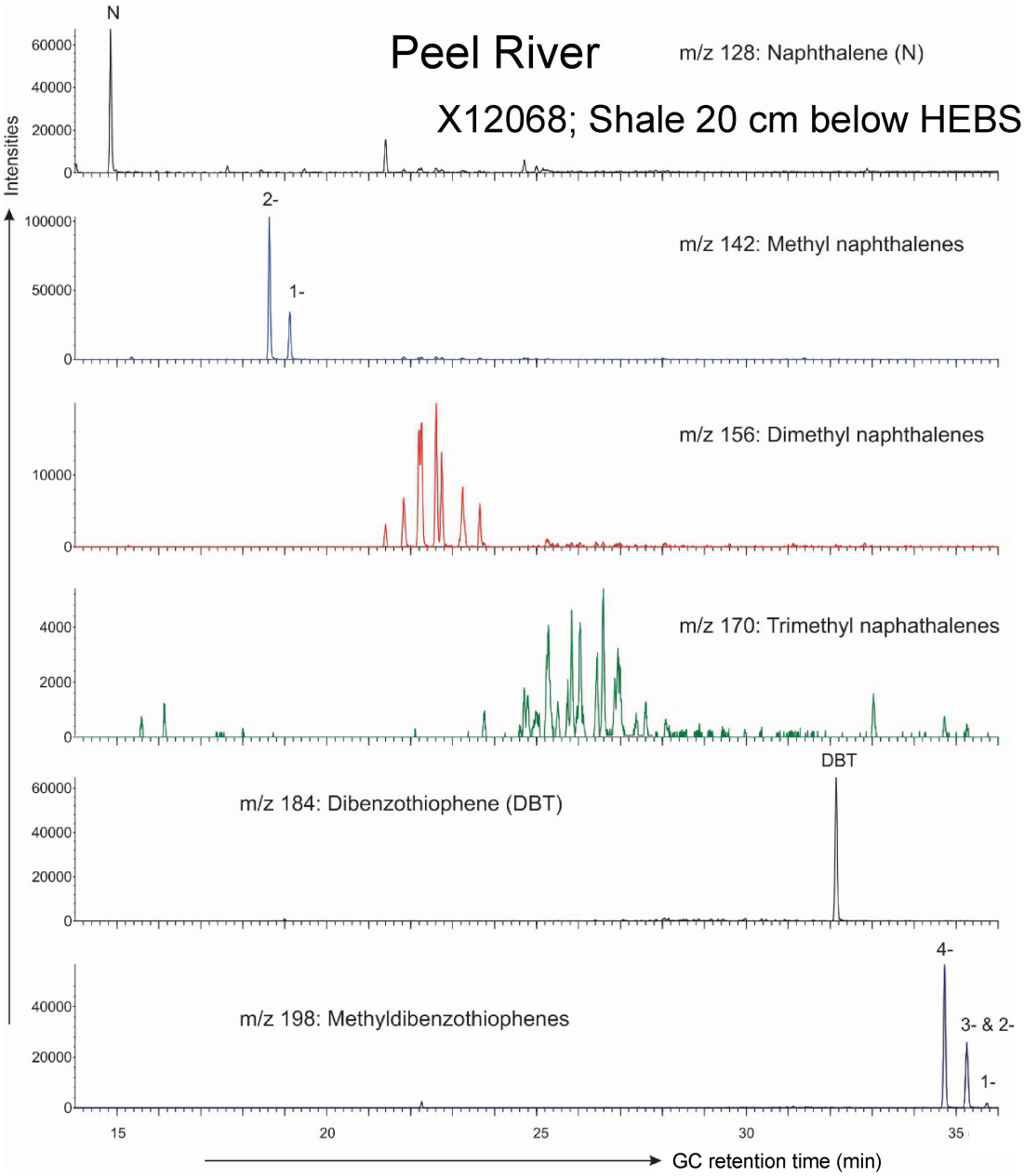

Figure 8. Mass chromatograms of a sample (X12068) of shale located 20 cm below the hyper-enriched black shale (HEBS) layer at the Peel River deposit, Yukon, showing the distributions of naphthalenes and dibenzothiophenes.

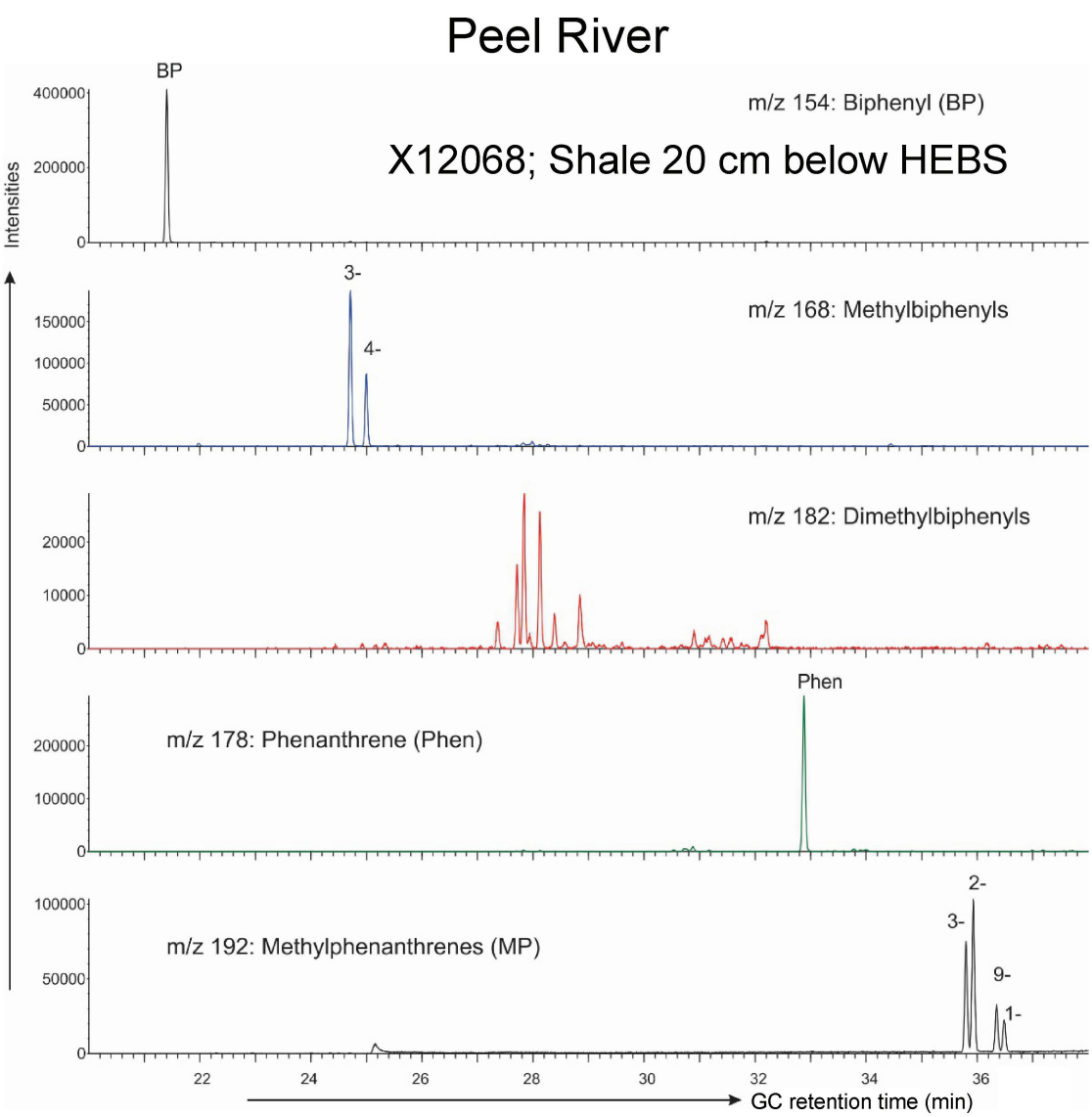

Figure 9. Mass chromatograms of a sample (X12068) of shale located 20 cm below the hyper-enriched black shale (HEBS) layer at the Peel River deposit, Yukon, showing the distributions of biphenyls and phenanthrenes.

burial. Gordey and Anderson (1993) attributed the heating to the intrusion of mid-Cretaceous granite plutons, which are widespread in the area. The high thermal maturity indicated for Nick based on the present study, as well as conodont colour alteration index (CAI; M. Orchard, unpub. rept., 1991) values (*see* below), indicates that the area may also have been subjected to anomalously high heat flow. The processes responsible for this heating are currently unknown, but possible explanations include imbricate thrust stacking (in the Howard's Pass district; Martel, 2017), crustal thinning, or alkalic mafic volcanism (Peter and Gadd, unpub. data, 2012). A detailed analysis of the thermal history and thermal maturity across and between the areas of focus is outside of the scope of the present study.

In addition to the Rock-Eval pyrolysis, organic petrography, and GC characteristics of SOM, there are other indicators of thermal maturity, including the conodont CAI (Epstein et al., 1977), and graptolite reflectance (Goodarzi and Norford, 1985). Conodonts are variably abundant in the rocks sampled in this study and can provide important biostratigraphic constraints (e.g. Gadd et al., 2020). Conodonts undergo sequential colour changes with increasing temperature (Epstein et al., 1977). Colour alteration begins at approximately 50°C and is cumulative and irreversible. In addition to recording thermal effects, CAI values are also logarithmically time dependent at any given temperature; conodonts subjected to low temperatures for long periods can yield higher CAI values than conodonts subjected to high temperatures for short periods. The CAI ranges from 1 to 6:

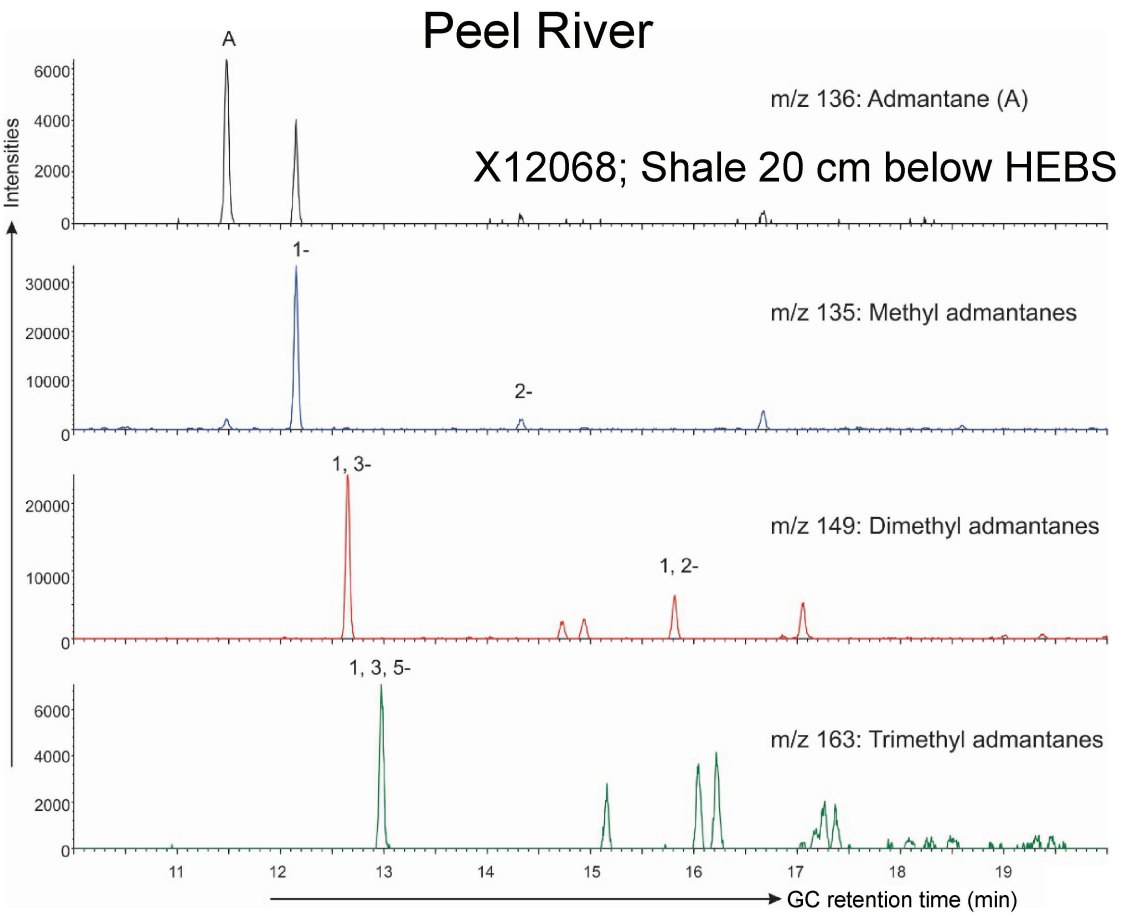

Figure 10. Mass chromatograms of a sample (X12068) of shale located 20 cm below the hyper-enriched black shale (HEBS) layer at the Peel River deposit, Yukon, showing the distributions of adamantanes.

1 = less than 50 to 80°C; 2 = 60 to 140°C; 3 = 110 to 200°C; 4 = 190 to 300°C; 5 = 300 to 480°C; and 6 = 360 to 550°C (Epstein et al., 1977); however, events such as regional and contact metamorphism and hydrothermal alteration can result in high(er) CAI values (up to 8) that do not reflect the burial temperatures given above (Rejebian et al., 1987). Graptolite reflectance has also been used in a similar manner to CAI (e.g. Goodarzi and Norford, 1985, 1989; Riediger et al., 1989).

The CAI values for our studied stratigraphic section at Nick range from 5 to 6 (M. Orchard, unpub. rept., 1991). Conodonts recovered from strata in the Howard's Pass district that are the focus of our study all have a CAI value of 5 (Goodarzi and Norford, 1985; Norford and Orchard, 1985; Goodfellow and Jonasson, 1986; Riediger et al., 1989), indicating temperatures of 300 to 480°C (Epstein et al., 1977). Indeed, the Goodarzi and Norford (1985) CAI value of 5 is for one sample of Road River Group shale from the main adit of the greater XY deposit (of which XY Central is a part), Howard's Pass district, very close to the XY Central samples used in our study. Martel et al. (2011) reported thermal maturity data (based on fossil data) for the central Mackenzie Mountains, and our data generally support their conclusion that, in the XY Central area, R_o equivalent maximum generally ranges between 3 and 4% for upper Cambrian to Middle Devonian strata (using the CAI conversion in Utting et al. (1989)); however, the data coverage of Martel et al. (2011) does not extend as far west as Nick or Peel River. W.D. Goodfellow and H.J. Geldsetzer (unpub. rept., 1995) report CAI values of 2 to 3 (with two samples giving an outlier CAI value of 4) for 15 samples of the Peel River HEBS and host rocks that we studied. These CAI data support our conclusion that the Peel River strata were subjected to lower temperatures than at Nick and XY Central. These differences likely reflect broad regional differences in thermal maturity. Peel River HEBS is approximately 100 km north-northwest of the Nick HEBS, and there are marked thermal maturity differences between them; however, the Monster River HEBS site, approximately 200 km west-southwest of the Peel River HEBS (Fig. 1), has CAI values of 2 to 3, similar to those at Peel River (T. Uyeno, unpub. rept., 1994). These differences may be attributable to differences in the structural regimes between the two sites (folds, faults).

Organic matter type

No steranes and terpanes, which are useful for elucidating depositional environments and organic inputs, were detected in any of the studied samples. Due to the severe thermal isomerization and destruction reactions, the PAHs in the Peel River samples contain limited information about the origin of the precursor organic matter, and cannot be used to elucidate the type(s) of deposited biomass; however, based on the Ordovician and Devonian ages of the shales and mudstones at the three sites, it is reasonable to assume that all of the original organic matter at XY Central, and most of it (by far) at Peel River and Nick was kerogen type II (algal and bacterial organic matter dominated by liptinite macerals; common in marine settings), with an average HI of 600 (e.g. Tissot and Welte, 1984). This HI value suggests that the original TOC content was approximately twice the present TOC content. Much of the organic carbon was likely converted to gaseous hydrocarbons and light hydrocarbon liquids and lost. Peel River and Nick HEBS also contain minor fossil woody terrestrial plant matter — type III kerogen — which typically generates gas.

Contamination

Considering the very high thermal maturity and the extremely low amounts of SOM extracted from the shale samples, many of the compounds detected appear to be contaminants introduced during sample collection and preparation. Although every effort was taken to minimize contamination, the C_{21} to C_{31} normal alkanes (*n*-alkanes) that dominate the GC-amenable components in some samples of mineralized and unmineralized shales from XY Central and Nick (Fig. 5, 6, and 7, respectively) likely originate from wax components that are widely used in consumer products (e.g. sample bags, wax pencils, felt markers, lip protectant, and sunscreen). Wax contamination of geological samples can overwhelm rock samples that contain very low amounts of pristine SOM (Jiang et al., 2014).

Any high molecular weight hydrocarbons originally present would have been converted to light and gaseous hydrocarbons via thermal cracking during burial metamorphism and/or regional heating (Peters et al., 2015). Plasticizers (peaks labelled 'pht' in Fig. 4b–d, 5a) are another type of contaminant detected in high abundances in the samples; this may be caused by using plastic sample bags. In addition to these identified contaminant types, a few other structurally unknown compounds were detected as major peaks on the TICs from GCMS analysis of the SOM samples (Fig. 4, 5, 6, and 7). Some may contain O and/or N atoms and may have been sourced from recent biomass or artificial materials.

The discussed contaminants dominate the TICs of most studied samples because pristine hydrocarbons derived from the organic matter in the samples via thermal maturation have undergone severe thermal stress and are either present at much lower concentrations or no longer present. C_{12} to C_{20} *n*-alkanes are detected as major compounds in some of the XY Central samples (Fig. 7). Unlike the C_{21} to C_{31} long-chain, high molecular weight *n*-alkanes that are likely waxy artefacts, the low molecular weight *n*-alkanes may be natural hydrocarbons formed in the shale during hydrothermal or regional heating events; however, their even-over-odd carbon preference distribution pattern seems to contradict their high maturity characteristics; therefore, it is not clear whether C_{12} to C_{20} *n*-alkanes in the XY Central samples are fossil hydrocarbons or artefacts.

The addition of activated copper grains to the solvent extracts containing the SOM failed to completely remove elemental sulfur in certain samples (HEBS and SEDEX mineralization, and also host shales and mudstones in both settings, which are unmineralized but can contain abundant framboidal pyrite; Gadd et al., 2016; Gadd and Peter, 2018). The sulfide in the rocks may have been oxidized to elemental sulfur during surface weathering (outcrop samples only) or during the solvent extraction process, and this may explain the presence of elemental sulfur detected by GCMS analysis in certain samples (peaks labelled S8 in Figs. 4, 5, and 6).

CONCLUSIONS

We studied the characteristics of organic matter in SEDEX and HEBS mineralization and unmineralized host rocks in the Selwyn Basin and correlative strata of the Richardson trough using Rock-Eval pyrolysis, organic petrography, and solvent extraction and GCMS analysis of the SOM in samples from the XY Central SEDEX deposit in the Howard's Pass district and the Nick and Peel River HEBS deposits in the Richardson trough. All samples have experienced extremely high thermal maturity (T_{max} up to 599°C), indicating that they contain low SOM, and Rock-Eval parameters S1, S2, HI, and OI values are low, whereas RC values are universally high. Mineral carbon values are low for all deposits studied. Pyrobitumen reflectance values range from 1.75 to 5.80%, corresponding to the dry gas and thermally over-mature stages of hydrocarbon generation.

Total ion and mass chromatograms from full-scan GCMS analyses of SOM reveal that all of the sterane and terpane biomarkers and other high molecular weight hydrocarbons have been lost due to thermal cracking, and many remaining peaks are likely due to contaminants introduced during sampling; however, differences in some Rock-Eval parameters (higher HI and lower RC at Peel River), GCMS spectra (PAHs and adamantanes present at Peel River, but absent at Nick and XY Central), organic petrographic characteristics (lower pyrobitumen reflectances at Peel River compared to Nick and XY Central), and evidence gleaned from other studies (lower CAI values at Peel River compared to Nick and XY Central; Goodarzi and Norford, 1985; Norford and Orchard, 1985; Goodfellow and Jonasson, 1986; Riediger et al., 1989; M. Orchard, unpub. rept., 1991; W.D. Goodfellow

and H.J. Geldsetzer, unpub. data, 1995) collectively indicate that the Peel River deposit experienced slightly lower thermal effects than Nick and XY Central.

The high degree of thermal maturity evidenced at all three study localities is in contrast with their low metamorphic grade and burial depths. Even at XY Central, a seafloor hydrothermal deposit, hydrothermal circulation is unlikely to have been the cause of overmaturation. Although the processes responsible for this heating are currently unknown, possible explanations include imbricate thrust stacking or alkalic mafic volcanism (in the Howard's Pass district) or crustal thinning (at all three localities). Further work to elucidate the thermal history of the study areas could use low-temperature thermochronology (e.g. Powell et al., 2019), perhaps on syngenetic to diagenetic fluorapatite, which is present at all three localities. Finally, we were unsuccessful in achieving our ultimate goal of determining the biomarker signatures of marine biota to determine their possible role in fixing metals to produce metal sulfide deposits.

ACKNOWLEDGMENTS

We thank Marina Milovic, Rachel Robinson, Richard Vandenberg, and Patricia Webster at the GSC laboratories in Calgary, Alberta, for organic geochemical and petrographic analyses. We also thank Keith Dewing and Jeremy Powell for their reviews, which improved the paper.

REFERENCES

ASTM International, 2011. ASTM D7708-11. Standard test method for microscopical determination of the reflectance of vitrinite dispersed in sedimentary rocks; Sec. 5, Volume 05.06 *in* Annual Book of ASTM Standards; ASTM International, West Conshohocken, Pennsylvania, p. 1–10. https://doi.org/10.1520/D7708-11

Becker, R.T., Gradstein, F.M., and Hammer, O., 2012. The Devonian period; Chapter 22 *in* The geological time scale 2012, (ed.) F.M. Gradstein, J.G. Ogg, M. Schmitz, and G. Ogg; Elsevier, Oxford, U.K., p. 559–601. https://doi.org/10.1016/B978-0-444-59425-9.00022-6

Behar F., Beaumont V., and De B. Penteado, H.L., 2001. Rock-Eval 6 technology: performances and developments; Oil and Gas Science and Technology, v. 56, no. 2, p. 111–134. https://doi.org/10.2516/ogst:2001013

Coveney, R.M., Jr., 1997. Metalliferous shales and the role of organic matter with examples from China, Poland, and the United States; *in* Ore genesis and exploration: the roles of organic matter, (ed.) J.S. Leventhal and T.H. Giordano; Reviews in Economic Geology, v. 9, p. 251–280. https://doi.org/10.5382/Rev.09.11

Curiale, J.A., 1986. Origin of solid bitumens, with emphasis on biological marker results; Organic Geochemistry, v. 10, no. 1–3, p. 559–580. https://doi.org/10.1016/0146-6380(86)90054-9

Dahl, J.E., Moldowan, J.M., Peters. K.E., Claypool, G.E., Rooney, M.A., Michael, G. E., Mello, M.R., and Kohnen, M.L., 1999. Diamondoid hydrocarbons as indicators of natural oil cracking; Nature, v. 399, p. 54–57. https://doi.org/10.1038/19953

Eisbacher, G.H., 1981. Sedimentary tectonic and glacial record in the Windermere Supergroup, Mackenzie Mountains, Northwestern Canada; Geological Survey of Canada, Paper 80-27, 40 p. https://doi.org/10.4095/119453

Epstein, A.G., Epstein, J.B., and Harris, L.D., 1977. Conodont color alteration—an index to organic metamorphism; United States Geological Survey, Professional Paper 995, 27 p.

Espitalié, J., 1986. Use of Tmax as a maturation index for different types of organic matter: comparison with vitrinite reflectance; *in* Thermal modelling in sedimentary basins, (ed.) J. Burrus; Editions Technip, Paris, p. 475–496.

Fraser, T.A., and Hutchinson, M.P., 2017. Lithogeochemical characterization of the Middle–Upper Devonian Road River Group and Canol and Imperial formations on Trail River, east Richardson Mountains, Yukon: age constraints and a depositional model for fine-grained strata in the Lower Paleozoic Richardson trough; Canadian Journal of Earth Sciences, v. 54, p. 731–765. https://doi.org/10.1139/cjes-2016-0216

Gadd, M.G. and Peter, J.M., 2018. Field observations, mineralogy and geochemistry of Middle Devonian Ni-Zn-Mo-PGE hyper-enriched black shale deposits; *in* Targeted Geoscience Initiative: 2017 report of activities, volume 1, (ed.) N. Rogers; Geological Survey of Canada, Open File 8358, p. 193–206. https://doi.org/10.4095/306475

Gadd, M.G., Layton-Matthews, D., Peter, J.M., and Paradis, S.J., 2016. The world-class Howard's Pass SEDEX Zn-Pb district, Selwyn Basin, Yukon. Part I: trace element compositions of pyrite record input of hydrothermal, diageneic, and metamorphic fluids to mineralization; Mineralium Deposita, v. 51, p. 319–342. https://doi.org/10.1007/s00126-015-0611-2

Gadd, M.G., Layton-Matthews, D., Peter, J.M., Paradis, S., and Jonasson, I.R., 2017. The world-class Howard's Pass SEDEX Zn-Pb district, Selwyn Basin, Yukon. Part II: the roles of thermochemical and bacteria sulfate reduction in metal fixation; Mineralium Deposita, v. 52, p. 405–419. https://doi.org/10.1007/s00126-016-0672-x

Gadd, M.G., Peter, J.M., Jackson, S.E., Yang, Z., and Petts, D., 2019. Platinum, Pd, Mo, Au and Re deportment in hyper-enriched black shale Ni-Zn-Mo-PGE mineralization, Peel River, Yukon, Canada; Ore Geology Reviews, v. 107, p. 600–614. https://doi.org/10.1016/j.oregeorev.2019.02.030

Gadd, M.G., Peter, J.M., Hnatyshin, D., Creaser, R., Gouwy, S., and Fraser, T., 2020. A Middle Devonian basin-scale precious metal enrichment event across northern Yukon: Geology, , v. 48, no. 3, p. 242–246. https://doi.org/10.1130/G46874.1

Gal, L.P., Allen, T.L., Hadlari, T., and Zantvoort, W.G., 2009. Petroleum systems elements; Chapter 10 *in* Regional geoscience Ssudies and petroleum potential, Peel Plateau and Plain, Northwest Territories and Yukon: Project Volume, (ed.) L.J. Pyle and A.L. Jones; Northwest Territories Geoscience Office and Yukon Geological Survey, NWT Open File 2009-02 and YGS Open File 2009-25, p. 477–549.

Goldhaber, M.B. and Kaplan, I.R., 1980. Mechanisms of sulfur incorporation and isotope fractionation during early diagenesis in sediments of the Gulf of California; Marine Chemistry, v. 9, no. 2, p. 95–143. https://doi.org/10.1016/0304-4203(80)90063-8

Goodarzi, F. and Norford, B.S., 1985, Graptolites as indicators of the temperature histories of rocks; Journal of the Geological Society, v. 142, no. 6, p. 1089–1099. https://doi.org/10.1144/gsjgs.142.6.1089

Goodarzi, F. and Norford, B.S., 1989. Variation of graptolite reflectance with depth of burial; International Journal of Coal Geology, v. 11, no. 2, p. 127–141. https://doi.org/10.1016/0166-5162(89)90002-5

Goodfellow, W.D., 2007. Base metal metallogeny of the Selwyn Basin, Canada; *in* Mineral resources of Canada: a synthesis of major deposit types, district metallogeny, the evolution of geological provinces, and exploration methods, (ed.) W.D. Goodfellow; Geological Association of Canada, Mineral Deposits Division, Special Publication No. 5, p. 553–579.

Goodfellow, W.D. and Jonasson, I.R., 1986. Environment of formation of the Howards Pass (XY) Zn-Pb deposit, Selwyn Basin, Yukon; *in* Mineral deposits of the northern Cordillera, (ed.) J.A. Morin; Canadian Institute of Mining and Metallurgy, Special Volume 37, p. 19–50.

Gordey, S.P., 2008. Geology, Selwyn Basin, (105J and 105K), Yukon; Geological Survey of Canada, Open File 5438, 3 sheets, 2 maps at 1:250 000 scale. https://doi.org/10.4095/225395

Gordey, S.P. and Anderson, R.G., 1993. Evolution of the northern Cordillera miogeocline, Nahanni map area (105I), Yukon and Northwest Territories; Geological Survey of Canada, Memoir 428, 214 p. https://doi.org/10.4095/183983

Gordey, S.P., 1988. Devonian-Mississippian clastic sedimentation and tectonism in the Canadian Cordilleran miogeocline; *in* Volume II, sedimentation; Devonian of the World: Proceedings of the 2nd international symposium of the Devonian system;, (ed.) N.J. McMillan, A.F. Embry, and D.J. Glass; Canadian Society of Petroleum Geologists, Memoir 14, p. 1–14.

Holman, A.I., Greenwood, P.F., Brocks, J.J., and Grice, K., 2014a. Effects of sulfide minerals on aromatic maturity parameters: laboratory investigation using micro-scale sealed vessel pyrolysis; Organic Geochemistry, v. 76, p. 270–277. https://doi.org/10.1016/j.orggeochem.2014.09.001

Holman, A.I., Grice, K., Greenwood, P.F., Böttcher, M.E., Walshe, J.L., and Evans, K. A., 2014b. New aspects of sulfur biogeochemistry during ore deposition from $\delta^{34}S$ of elemental sulfur and organic sulfur from the Here's Your Chance Pb/Zn/Ag deposit; Chemical Geology, v. 387, p. 126–132. https://doi.org/10.1016/j.chemgeo.2014.08.025

Holman, A.I., Grice, K., Jaraula, C.M.B., and Schimmelmann, A., 2014c. Bitumen II from the Paleoproterozoic *Here's Your Chance* Pb/Zn/Ag deposit: implications for the analysis of depositional environment and thermal maturity of hydrothermally-https://doi.org/10.1016/j.gca.2014.04.035

Hyndman, R.D., 2010. The consequences of Canadian Cordillera thermal regime in recent tectonics and elevation: a review; Canadian Journal of Earth Sciences, v. 47, p. 621–632. https://doi.org/10.1139/E10-016

Hulbert, L.J., Gregoire, D.C., Paktunc, D., and Carne, R.C., 1992, Sedimentary nickel, zinc, and platinum-group-element mineralization in Devonian black shales at the Nick property, Yukon, Canada: anew deposit type; Exploration and Mining Geology, v. 1, p. 39–62.

International Committee for Coal and Organic Petrology (ICCP), 1993. International handbook of coal petrography, 3rd Supplement to 2nd ed.; International Committee for Coal and Organic Petrology, 146 p.

Issler, D.R., Grist, A., and Stasiuk, L., 2005. Post-Early Devonian thermal constraints on hydrocarbon source rock maturation in the Keele tectonic zone, Tulita area, NWT, Canada, from multi-kinetic apatite fission track thermochronology, vitrinite reflectance and shale compaction; Bulletin of Canadian Petroleum Geology, v. 53, p. 405–431, https://doi.org/10.2113/53.4.405

Jacob, H., 1989. Classification, structure, genesis and practical importance of natural solid oil bitumen ("migrabitumen"); International Journal of Coal Geology. v. 11, no. 1, p. 65–79. https://doi.org/10.1016/0166-5162(89)90113-4

Jiang, C., Pyle, L.J., and Gal, L.P., 2014. Organic geochemistry of petroleum hydrocarbons in Middle to Upper Devonian outcrop samples from Mackenzie Plain area; Geological Survey of Canada, Open File 7600 and Northwest Territories Geoscience Office, Open File 2014-05, 48 p. https://doi.org/10.4095/295194

Jiang, C., Chen, Z., Lavoie, D., Percival, J.B., and Kabanov, P., 2017. Mineral carbon MinC(%) from Rock-Eval analysis as a reliable and cost-effective measurement of carbonate contents in shale source and reservoir rocks; Marine and Petroleum Geology, v. 83, p. 184–194. https://doi.org/10.1016/j.marpetgeo.2017.03.017

Johnson, C.A., Slack, J.F., Dumoulin, J.A., Kelley, K.D., and Falck, H., 2018. Sulfur isotopes of host strata for Howards Pass (Yukon-Northwest Territories) Zn-Pb deposits implicate anaerobic oxidation of methane, not basin stagnation; Geology, v. 46, no. 7, p. 619–622. https://doi.org/10.1130/G40274.1

Kawasaki, K. and Symons, D.T.A., 2012. Paleomagnetism of the Howards Pass Zn-Pb deposits, Yukon, Canada; Geophysics Journal International, v. 190, no. , p. 217–229. https://doi.org/10.1111/j.1365-246X.2012.05484.x

Kelley, K.D., Selby, D., Falck, H., and Slack, J.F., 2017. Re-Os systematics and age of pyrite associated with stratiform Zn-Pb mineralization in the Howards Pass district, Yukon and Northwest Territories, Canada; Mineralium Deposita, v. 52, p. 317–335.

Kirkham, G., Dunning, J., and Schleiss, W., 2012. Update for Don deposit mineral resource estimate, Howard's Pass property, eastern Yukon, Selwyn Resources Ltd.; NI 43–101 Technical Report, 145 p.

Kus, J., Araujo, C. V., Borrego, A.G., Flores, D., Hackley, P.C., Hámor-Vidó, M., Kalaitzidis, S., Kommeren, C.J., Kwiecińska, B., Mastalerz, M., Mendonça Filho, J.G., Menezes, T.R., Misz-Kennan, M., Nowak, G.J., Petersen, H.I., Rallakis, D., Suárez-Ruiz, I., Sýkorová, I., and Životić, D., 2017. Identification of alginite and bituminite in rocks other than coal. 2006, 2009, and 2011 round robin exercises of the ICCP Identification of Dispersed Organic Matter Working Group; International Journal of Coal Geology, v. 178, p. 26–38. https://doi.org/10.1016/j.coal.2017.04.013

Lane, L.S., 2007. Devonian–Carboniferous paleogeography and orogenesis, northern Yukon and adjacent arctic Alaska; Canadian Journal of Earth Sciences, v. 44, p. 679–694. https://doi.org/10.1139/e06-131

Leventhal, J.S. and Giordano, T.H., 1997. The nature and roles of organic matter associated with ores and ore-forming systems: an introduction; *in* Ore genesis and exploration: the roles of organic matter, (ed.) J.S. Leventhal and T.H. Giordano; Reviews in Economic Geology, v. 9, p. 1–26. https://doi.org/10.5382/Rev.09.01

Magnall, J.M., Gleeson, S. A., Stern, R.A., Newton, R.J., Poulton, S.W., and Paradis, S., 2016. Open system sulphate reduction in a diagenetic environment – isotopic analysis of barite ($\delta^{34}S$ and $\delta^{18}O$) and pyrite ($\delta^{34}S$) from the Tom and Jason Late Devonian Zn–Pb–Ba deposits, Selwyn Basin, Canada; Geochimica et Cosmochimica Acta, v. 180, p. 146–163. https://doi.org/10.1016/j.gca.2016.02.015

Martel, E. 2015. The structural model for Howard's Pass Pb-Zn district, Northwest Territories: grounds for re-interpretation; Northwest Territories Geological Survey, NWT Open File 2015-01, 54 p.

Martel, E., 2017. The importance of structural mapping in ore deposits–A new perspective on the Howard's Pass Zn-Pb district, Northwest Territories, Canada; Economic Geology, v. 112, no. 6, p. 1285–1304. https://doi.org/10.5382/econgeo.2017.4510

Martel, E., MacNaughton, R.B. and Fischer, B.J., 2011. Metamorphism and thermal maturity; Chapter 6 *in* Geology of the central Mackenzie Mountains of the northern Canadian Cordillera, Sekwi Mountain (105P), Mount Eduni (106A), and northwestern Wrigley Lake (95M) map-areas, Northwest Territories, (ed.) E. Martel, E.C. Turner, and B.J. Fischer; Northwest Territories Geological Survey, NWT Special Volume 1, p. 251–254.

Morganti, J. M., 1979. The geology and ore deposits of the Howards Pass area, Yukon and Northwest Territories: the origin of basal sedimentary stratiform sulphide deposits: Unpub. Ph.D. thesis, University of British Columbia, 351 p.

Morrow, D.W., 1999. Lower Paleozoic stratigraphy of northern Yukon Territory and northwestern District of Mackenzie; Geological Survey of Canada, Bulletin 538, 202 p. https://doi.org/10.4095/210998

Nelson, J. and Colpron, M., 2007. Tectonics and metallogeny of the British Columbia, Yukon and Alaskan Cordillera, 1.8 Ga to the present; *in* Mineral deposits of Canada: a synthesis of major deposit types, district metallogeny, the evolution of geological provinces, and exploration methods, (ed.) W.D. Goodfellow; Geological Association of Canada, Mineral Deposits Division, Special Publication No. 5, p. 755–791.

Norford, B. and Orchard, M., 1985. Early Silurian age of rocks hosting lead-zinc mineralization at Howards Pass, Yukon Territory and District of Mackenzie; Geological Survey of Canada, Paper 83-18, 35 p. https://doi.org/10.4095/120311

Norris, A.W., 1985. Stratigraphy of Devonian outcrop belts in northern Yukon Territory and northwestern District of Mackenzie (Operation Porcupine area); Geological Survey of Canada, Memoir 410, 81 p. https://doi.org/10.4095/120309

Obermajer, M., Stewart, K. R., and Dewing, K. 2007. Geological and geochemical data from the Canadian Arctic Islands, part II: Rock-Eval/TOC data. Geological Survey of Canada, Open File 5459, 27 p., 1 CD-ROM. https://doi.org/10.4095/223457

Peter, J.M., Layton-Matthews, D., Gadd, M.G., Gill, S., Baker, S., Plett, S., and Paradis, S.J., 2015. Application of visible-near infrared and short wave infrared spectroscopy to SEDEX deposit exploration in the Selwyn Basin, Yukon; *in* Targeted Geoscience Initiative 4: Sediment-hosted Zn-Pb (±Ag, ±Ba) deposits: processes and implications for exploration; Geological Survey of Canada, Open File 7838, p. 152–172. https://doi.org/10.4095/296336

Peters, K.E., 1986. Guidelines for evaluating petroleum source rock using programmed pyrolysis; AAPG Bulletin, v. 70, p. 318–320. https://doi.org/10.1306/94885688-1704-11D7-8645000102C1865D

Peters, K.E. and Cassa, M.R., 1994. Applied source rock geochemistry; *in* The petroleum system–from source to trap, (ed.) L.B. Magoon and W.G. Dow; American Association of Petroleum Geologists, Memoir 60, p. 93–120.

Peters, K.E., Walters, C.C., and Moldowan, J.M., 2005. The biomarker guide, volume 2: biomarkers and isotopes in petroleum systems and earth history; Cambridge University Press, U.K., 700 p.

Pickel, W., Kus, J., Flores, D., Kalaitzidis, S., Christanis, K., Cardott, B.J., Misz-Kennan, M., Rodrigues, S., Hentschel, A., Hamor-Vido, M., Crosdale, P., and Wagner, N., 2017. Classification of liptinite – ICCP system 1994; International Journal of Coal Geology, v. 169, p. 40–61. https://doi.org/10.1016/j.coal.2016.11.004.

Powell, J.W., Issler, D.R., Schneider, D.A., Fallas, K.M., and Stockli, D.F., 2019. Thermal history of the Mackenzie Plain, Northwest Territories, Canada: insights from low-temperature thermochronology of the Devonian Imperial Formation; GSA Bulletin, v. 132, p. 767–783. https://doi.org/10.1130/B35089.1

Pratt, L.M., and Warner, M.C., 1997. Roles of organic matter in shale- and carbonate-hosted base metal deposits; *in* Ore genesis and exploration: the roles of organic matter, (ed.) J.S. Leventhal and T.H. Giordano; Reviews in Economic Geology, v. 9, p. 281–300. https://doi.org/10.5382/Rev.09.12

Pugh, D.C., 1983. Pre-Mesozoic geology in the subsurface of Peel River map area, Yukon Territory and District of Mackenzie; Geological Survey of Canada, Memoir 401, 61 p. https://doi.org/10.4095/119498

Rejebian, V.A., Harris, A.G., and Huebner, J.S., 1987. Conodont color and textural alteration; an index to regional metamorphism, contact metamorphism, and hydrothermal alteration; GSA Bulletin, v. 99, no. 4, p. 471–479. https://doi.org/10.1130/0016-7606(1987)99%3C471:CCATAA%3E2.0.CO;2

Riediger, C., Carrelli, G.G., and Zonneveld, J.-P., 2004. Hydrocarbon source rock characterization and thermal maturity of the Upper Triassic Baldonnel and Pardonet formations, northeastern British Columbia, Canada; Bulletin of Canadian Petroleum Geology, v. 52, no. 4, p. 277–301. https://doi.org/10.2113/52.4.277

Riediger, C., Goodarzi, F., and Macqueen, R.W., 1989. Graptolites as indicators of regional maturity in lower Paleozoic sediments, Selwyin Basin, Yukon and Northwest Territories, Canada; Canadian Journal of Earth Sciences, v. 26, no. 10, p. 2003–2015. https://doi.org/10.1139/e89-169

Schmidt, J.S., Menezes, T.R., Souza, I.V.A.F., Spigolon, A.L.D., Pestilho, A.L.S., and Coutinho, L.F.C., 2019. Comments on empirical conversion of solid bitumen reflectance for thermal maturity evaluation; International Journal of Coal Geology, v. 201, p. 44–50. https://doi.org/10.1016/j.coal.2018.11.012

Strauss, J.V., Fraser, T., Melchin, M.J., Allen, T.J., Malinowski, J., Feng, X, Taylor, J.F., Day, J., Gill, B.C., and Sperling, E.A., 2020. The Road River Group of northern Yukon Canada: early Paleozoic deep-water sedimentation within the Great American Carbonate Bank; Canadian Journal of Earth Sciences, e-First article. https://doi.org/10.1139/cjes-2020-0017

Taylor, G.H., Teichmüller; M., Davis, A., Diessel, C.F.K., Littke, R., and Robert, P. (eds.), 1998. Organic petrology; Gebrüder Borntraeger, Berlin, Germany, 704 p.

Tissot, B.P., and Welte, D.H., 1984. Petroleum formation and occurrence: a new approach to oil and gas exploration; Springer Verlag, Berlin, Germany, 699 p. https://doi.org/10.1007/978-3-642-96446-6

Utting, J., Goodarzi, F., Dougherty, B.J., and Henderson, C.M., 1989. Thermal maturity of Carboniferous and Permian rocks of the Sverdrup Basin, Canadian Arctic Archipelago; Geological Survey of Canada, Paper 89-19, 20 p. https://doi.org/10.4095/127356

Yukon Geological Survey, 2020. XY deposits (105I 012) record summary, Yukon mineral occurrence database; Government of Yukon, Yukon Geological Survey. <http://data.geology.gov.yk.ca/Occurrence/13388#Info> [accessed December 18, 2019]